Aquatic Botany

The plasticity of the photosynthetic apparatus and antioxidant responses are critical for the dispersion of Rhizophora mangle along a salinity gradient

--Manuscript Draft--

Manuscript Number:	AQBOT-D-22-00075R2
Article Type:	Research Paper
Keywords:	antioxidant metabolism; Climate change; mangroves; photosynthetic yield
Corresponding Author:	Milton Lima Neto, Ph.D UNESP: Universidade Estadual Paulista Julio de Mesquita Filho São Vicente, São Paulo BRAZIL
First Author:	Bruno Silva
Order of Authors:	Bruno Silva
	Ana Lobo
	Heloisa Saballo
	Milton Lima Neto, Ph.D
Abstract:	The physiological mechanisms responsible for salinity tolerance in Rhizophora mangle remain unclear. Moreover, the effects of climate change on the distribution and abundance of mangrove forests are unknown. Thus, to elucidate the possible factors responsible for saline tolerance in this species, we investigated the growth and physiological parameters in young plants cultivated in a saline gradient (0, 10, 35, and 70 ppt). Biometric indicators, water status parameters, cell integrity, ions concentrations in leaves and roots, pigment concentrations, chlorophyll a fluorescence, oxidative stress indicators, and antioxidant enzyme activities were evaluated. The results showed that R. mangle could grow in the absence (0 ppt) or moderate salinity (10 ppt). However, by increasing the salinity to sea level (35 ppt), the growth and development decreased compared to plants grown at ten ppt. In hypersalinity (70 ppt), plant growth and development are severely hampered. Under hypersalinity, the increased concentration of H2O2 promoted lipid peroxidation and membrane damage. The chlorophyll contents decreased, and accessory pigment concentrations increased. Moreover, the modulation of the quantum yield of PSII and the antioxidant system was crucial to avoiding photoinhibition and salinity tolerance in R. mangle.
Suggested Reviewers:	Kandasamy Kathiresan kathiresan57@gmail.com
	Kandasamy Saravanakumar saravana732@gmail.com
	Wenqing Wang wenqing2001@hotmail.com
	M. Adame f.adame@griffith.edu.au
Opposed Reviewers:	
Response to Reviewers:	All the minor suggestions, found as comments in the pdf file, were accepted and are highlighted in yellow in the file “Revised manuscript (with changes marked)”.

São Vicente, 14th November, 2022

Dear Dr. Thomas Wernberg,
Editor-in-Chief of Aquatic Botany.

Thank you for the valuable comments. We greatly appreciate the time and effort put forth by reviewers and editor to improve our paper. If any response are unclear or you wish additional changes, please let us know.

All the minor suggestions, found as comments in the pdf file, were accepted and are highlighted in yellow in the file “Revised manuscript (with changes marked)”.

Sincerely,

Dr. Milton C. Lima Neto
milton.lima-neto@unesp.br

Response to reviewers

All the minor suggestions, found as comments in the pdf file, were accepted and are highlighted in yellow in the file “Revised manuscript (with changes marked)”.

HIGHLIGHTS

- The plasticity of the photosynthetic metabolism is crucial for salinity tolerance in *R. mangle*
- *R. mangle* grows well in non-saline conditions
- 10 ppt NaCl provided the best growth condition for *R. mangle*
- Hypersalinity inhibits growth by causing an oxidative burst and reducing photosynthesis.
- *R. mangle* responds as a facultative halophyte

Abstract – The physiological mechanisms responsible for salinity tolerance in *Rhizophora mangle* remain unclear. Moreover, the effects of climate change on the distribution and abundance of mangrove forests are unknown. Thus, to elucidate the possible factors responsible for saline tolerance in this species, we investigated the growth and physiological parameters in young plants cultivated in a saline gradient (0, 10, 35, and 70 ppt). Biometric indicators, water status parameters, cell integrity, ions concentrations in leaves and roots, pigment concentrations, chlorophyll *a* fluorescence, oxidative stress indicators, and antioxidant enzyme activities were evaluated. The results showed that *R. mangle* could grow in the absence (0 ppt) or moderate salinity (10 ppt). However, by increasing the salinity to sea level (35 ppt), the growth and development decreased compared to plants grown at ten ppt. In hypersalinity (70 ppt), plant growth and development are severely hampered. Under hypersalinity, the increased concentration of H_2O_2 promoted lipid peroxidation and membrane damage. The chlorophyll contents decreased, and accessory pigment concentrations increased. Moreover, the modulation of the quantum yield of PSII and the antioxidant system was crucial to avoiding photoinhibition and salinity tolerance in *R. mangle*.

Figure1

Click here to access/download;Figure;Fig1.png

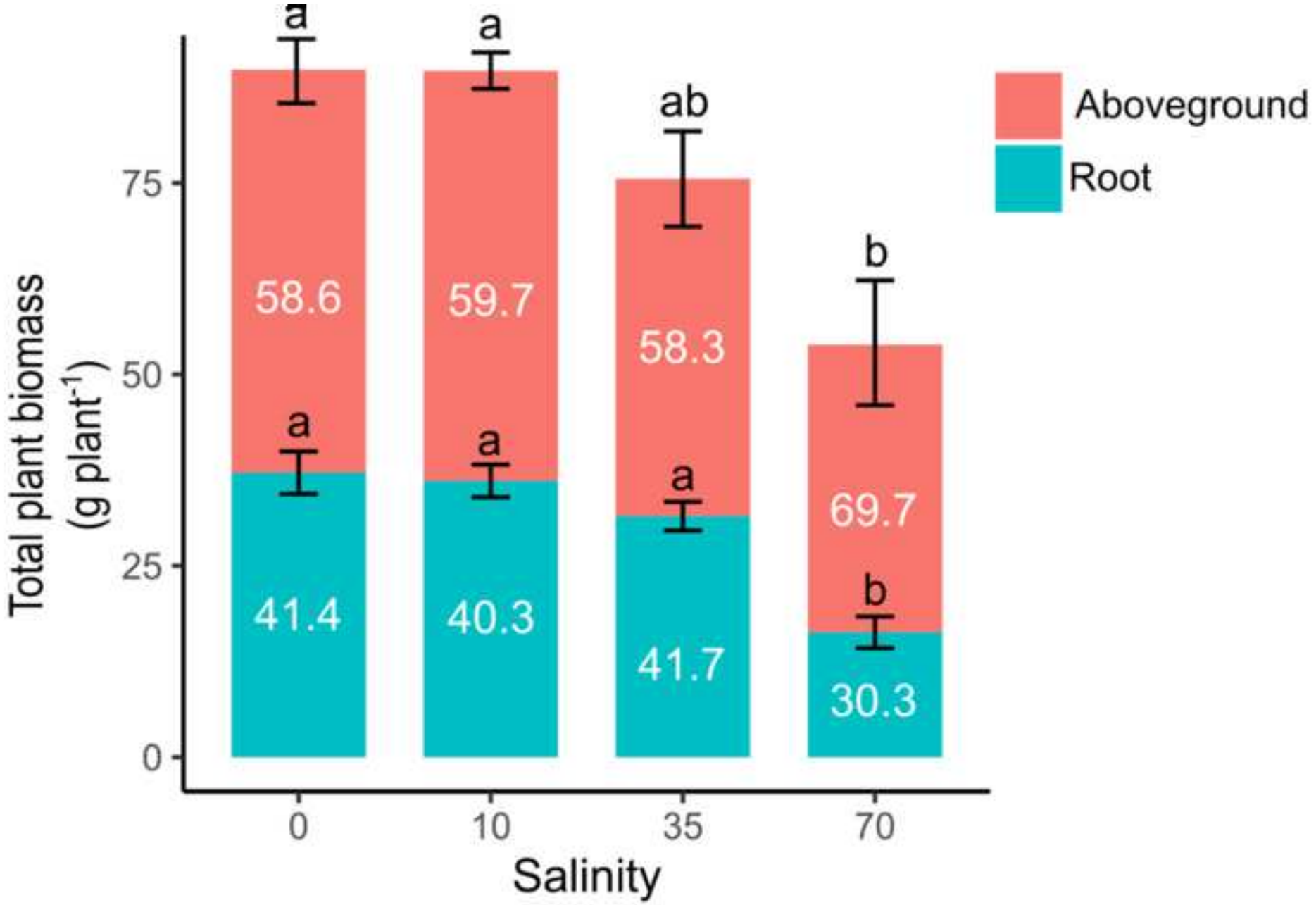

Figure2

Click here to access/download;Figure;Fig2.png

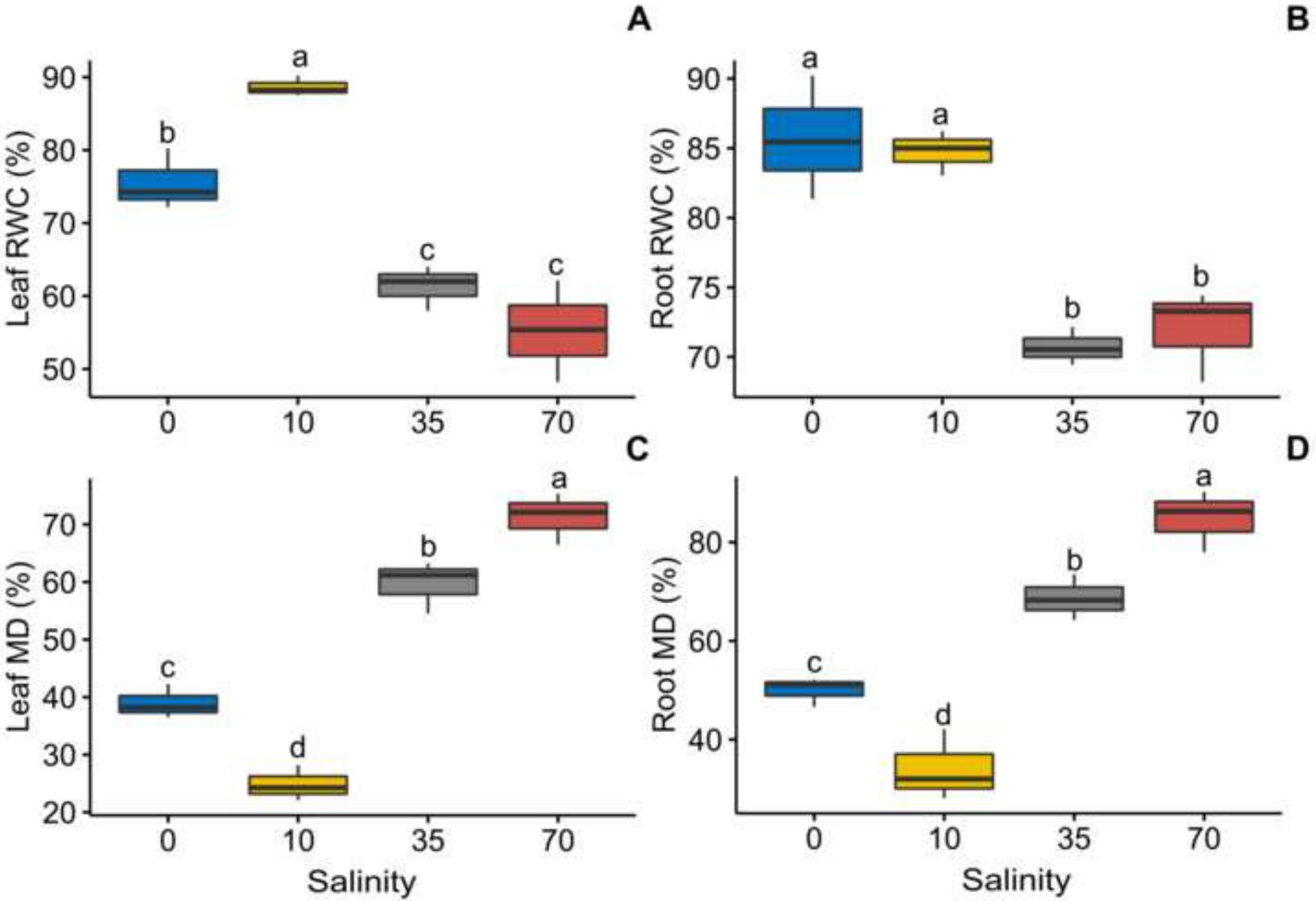

Figure3

Click here to access/download;Figure;Fig3.png

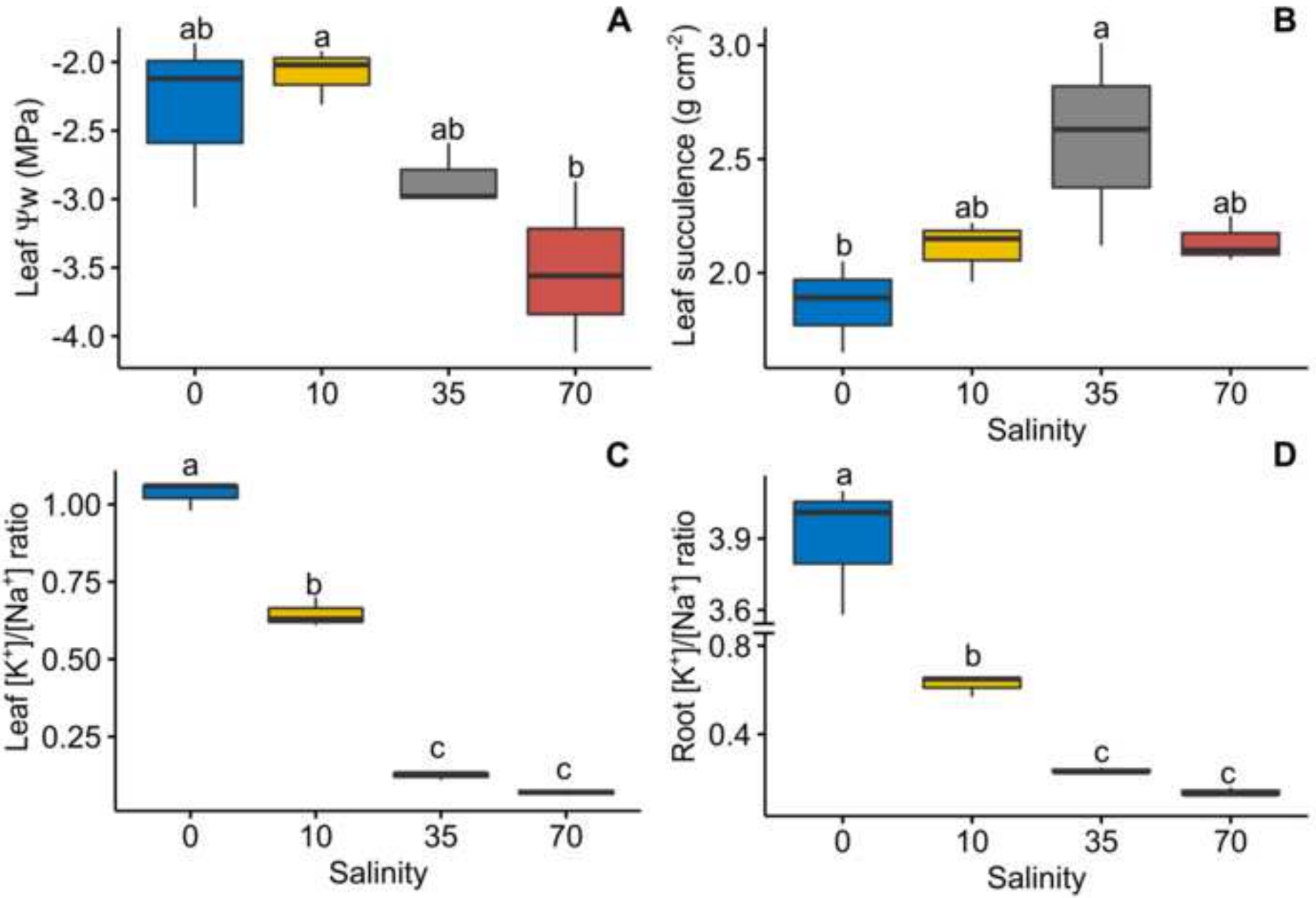

Figure4

Click here to access/download;Figure;Fig4.png

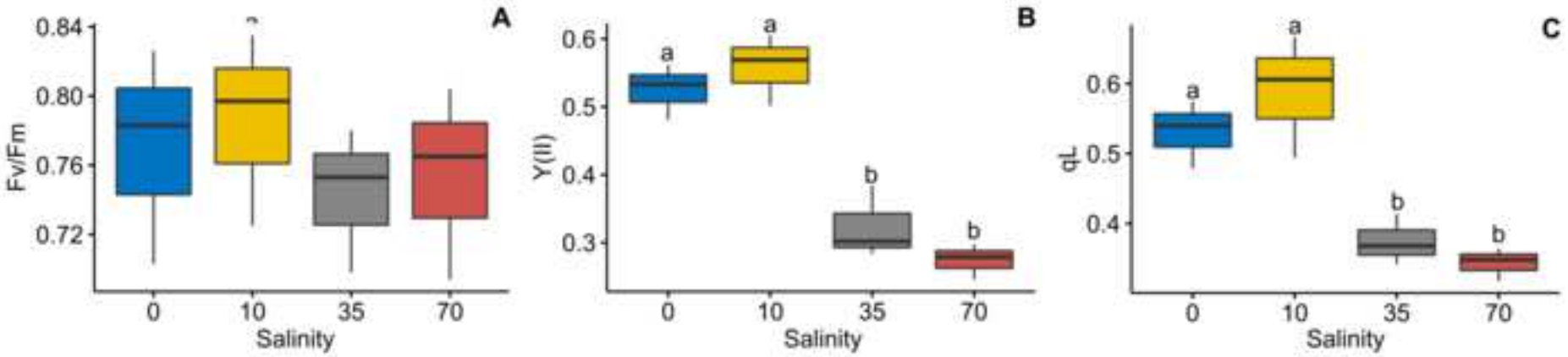

Figure5

Click here to access/download;Figure;Fig5.png

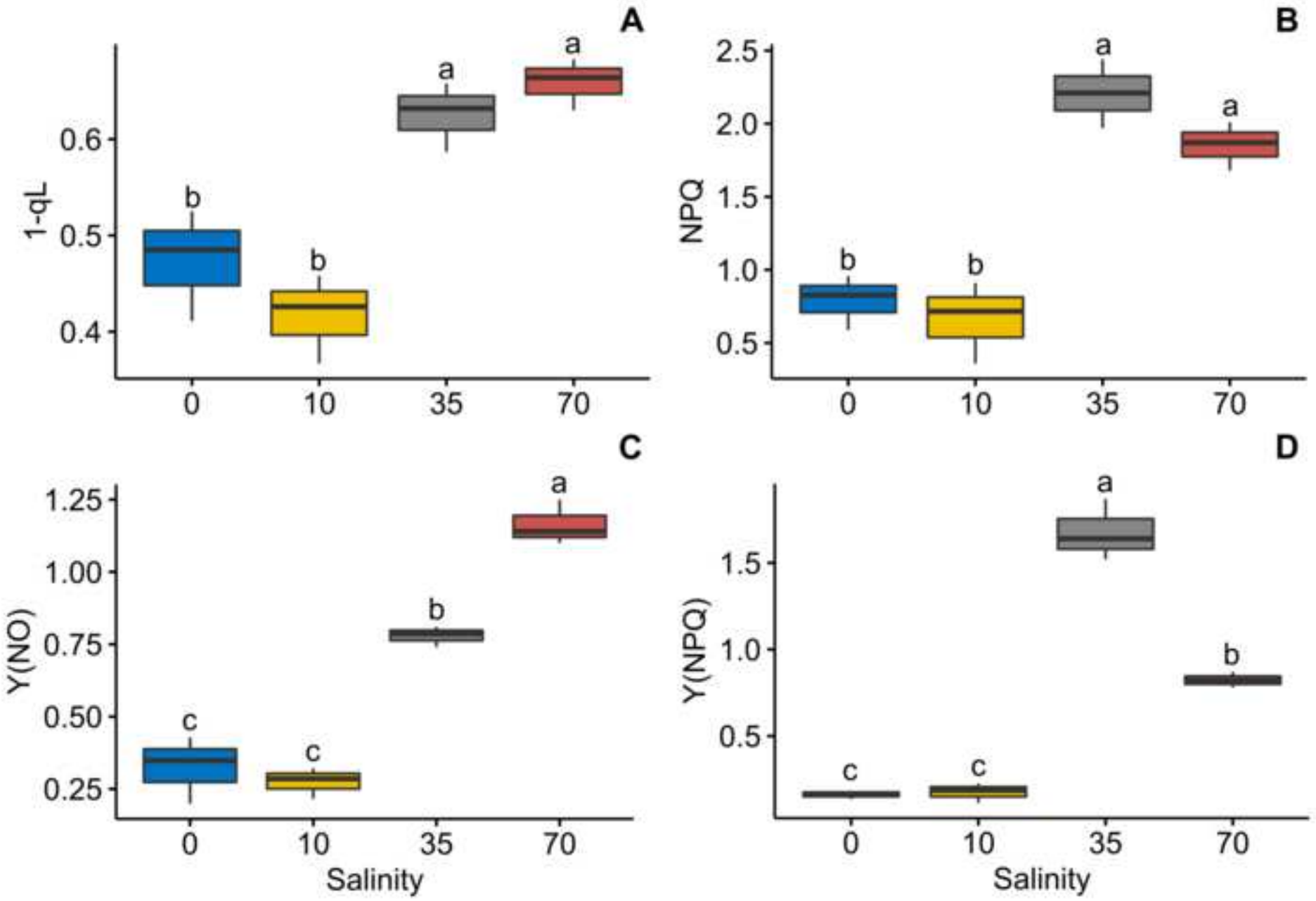

Table 1: Plant height, stem diameter, leaf area and number of leaves of *Rhizophora mangle* exposed to salinity levels in a growth chamber. Values represent the mean ± SD of five biological replicates (n = 5). According to Tukey's test, different letters represent significant differences between treatments ($P \leq 0.05$)

	0	**10**	**35**	**70**
Plant height (cm plant^{-1})	48.84 ± 1.73a	51.85 ± 1.96a	40.42 ±1.08b	36.06 ± 1.52b
Stem diameter (cm plant^{-1})	8.20 ± 0.66b	10.30 ± 0.67b	13.27 ± 0.44a	13.04 ± 0.48a
Leaf area (cm^2)	43.29 ± 2.58a	42.68 ± 2.87ab	33.68 ± 1.27bc	24.78 ± 1.03c
Number of leaves plant^{-1}	14.00 ± 0.58a	12.33 ± 0.33ab	10.67 ± 0.67b	7.67 ± 0.33c

Table 2: Total chlorophyll content, chlorophyll a/b ratio, carotenoids and anthocyanin contents in leaves of *Rhizophora mangle* exposed to increasing salinity. Values represent the mean ± SD of five biological replicates (n = 5). According to Tukey's test, different letters represent significant differences among treatments ($P \leq 0.05$).

	0		**10**		**35**		**70**	
Total Chl (mg g^{-1} FM)	99.21	±7.75 a	94.95	±6.97 a	67.85	±1.50 b	56.52	±2.62 b
Chl a/Chl b ratio	2.40	±0.30 a	2.00	±0.03 a	1.38	±0.08 b	1.53	±0.06 b
Carotenoids (mg g^{-1} FM)	95.54	±3.19 c	152.16	±9.20 b	174.60	±4.45 b	193.54	±4.70 a
Anthocyanin (mg g^{-1} FM)	0.98	±0.07 b	1.19	±0.04 b	2.01	±0.07 a	2.28	±0.14 a

Table 3: Contents of TBARS (lipid peroxidation) and H_2O_2, and the activities of superoxide dismutase, ascorbate peroxidase and catalase in leaves of *Rhizophora mangle* exposed to increasing salinity. Values represent the mean ± SD of five biological replicates (n = 5). According to Tukey's test, different letters represent significant differences among treatments ($P \leq 0.05$).

	0		**10**		**35**		**70**	
TBARS content (nmol MDA-TBA g^{-1} FM)	42.91	±4.70 c	85.39	±4.08 b	97.40	±2.65 ab	106.09	±3.99 a
H_2O_2 content (ηmol g^{-1} FM)	12.04	±0.38 c	30.74	±1.14 b	44.53	±2.00 a	47.12	±0.52 a
SOD activity (U mg^{-1} protein min^{-1})	2.58	±0.40 c	3.87	±0.38 bc	5.55	±0.32 ab	6.34	±0.45 a
APX activity (µmol mg^{-1} protein min^{-1})	0.81	±0.09 c	2.76	±0.20 b	3.87	±0.37 a	1.04	±0.02 c
CAT activity (µmol mg^{-1} protein min^{-1})	95.54	±3.19 c	152.16	±9.20 b	174.60	±4.45 ab	193.54	±4.70 a

Table 3: Contents of TBARS (lipid peroxidation) and H_2O_2, and the activities of superoxide dismutase, ascorbate peroxidase and catalase in leaves of *Rhizophora mangle* exposed to increasing salinity. Values represent the mean ± SD of five biological replicates (n = 5). According to Tukey's test, different letters represent significant differences among treatments ($P \leq 0.05$).

	0		**10**		**35**		**70**	
TBARS content (nmol MDA-TBA g^{-1} FM)	42.91	±4.70 c	85.39	±4.08 b	97.40	±2.65 ab	106.09	±3.99 a
H_2O_2 content (ηmol g^{-1} FM)	12.04	±0.38 c	30.74	±1.14 b	44.53	±2.00 a	47.12	±0.52 a
SOD activity (U mg^{-1} protein min^{-1})	2.58	±0.40 c	3.87	±0.38 bc	5.55	±0.32 ab	6.34	±0.45 a
APX activity (µmol mg^{-1} protein min^{-1})	0.81	±0.09 c	2.76	±0.20 b	3.87	±0.37 a	1.04	±0.02 c
CAT activity (µmol mg^{-1} protein min^{-1})	95.54	±3.19 c	152.16	±9.20 b	174.60	±4.45 ab	193.54	±4.70 a

Declaration of interests

The authors declare that they have no known competing financial interests or personal relationships that could have appeared to influence the work reported in this paper.

figS1

figS2

tableS1

Click here to access/download

e-Component

STable1.odt

tableS2

Click here to access/download
e-Component
STable2.odt

Conflict of Interest

All authors declare that they have no conflicts of interest.

The plasticity of the photosynthetic apparatus and antioxidant responses are critical for the dispersion of *Rhizophora mangle* along a salinity gradient

Bruno Pereira Silva[a], Heloisa Maria Saballo[a], Ana Karla Moreira Lobo[b], Milton Costa Lima Neto[a*]

[a]São Paulo State University (UNESP). Biosciences Institute, Coastal Campus, São Vicente – SP, Brazil. PO box 73601 Zip Code: 11380-972

[b]Lancaster Environment Centre, Lancaster University, Lancaster, UK

*MCLN is the corresponding author. email: milton.lima-neto@unesp.br. Praça Infante Dom Henrique s/n. ZIP code 11.330-900, Parque Bitarú, São Vicente, SP, Brasil.

Abstract – The physiological mechanisms responsible for salinity tolerance in *Rhizophora mangle* remain unclear. Moreover, the effects of climate change on the distribution and abundance of mangrove forests are unknown. Thus, to elucidate the possible factors responsible for saline tolerance in this species, we investigated the growth and physiological parameters in young plants cultivated in a saline gradient (0, 10, 35, and 70 ppt). Biometric indicators, water status parameters, cell integrity, ions concentrations in leaves and roots, pigment concentrations, chlorophyll *a* fluorescence, oxidative stress indicators, and antioxidant enzyme activities were evaluated. The results showed that *R. mangle* could grow in the absence (0 ppt) or moderate salinity (10 ppt). However, by increasing the salinity to sea level (35 ppt), the growth and development decreased compared to plants grown at ten ppt. In hypersalinity (70 ppt), plant growth and development are severely hampered. Under hypersalinity, the increased concentration of H_2O_2 promoted lipid peroxidation and membrane damage. The chlorophyll contents decreased, and accessory pigment concentrations increased. Moreover, the modulation of the quantum yield of PSII and the antioxidant system was crucial to avoiding photoinhibition and salinity tolerance in *R. mangle.*

Keywords: antioxidant metabolism; climate change; mangroves; photosynthetic yield

Abbreviations: APX - ascorbate peroxidase; CAT – catalase; Fv/Fm – the potential yield of PSII; MD – membrane damage; NPQ – non-photochemical quenching; PPFD - photosynthetic photon flux density; PSII - photosystem II; PPFD - photosynthetic photon flux density, ppt – part per thousand; RWC – relative water content; TCC – total chlorophyll content; qL - estimation of the fraction of open PSII centers based on the lake model, rcf –

relative centrifuge force, SOD - superoxide dismutase, TBARS - thiobarbituric acid reactive substances; TCC – total chlorophyll; Y(II) – effective quantum yield of photosystem II; YNO – on-regulated non-photochemical energy loss; YNPQ – regulated non-photochemical energy loss

1 Introduction

Mangrove forests are distributed worldwide in tropical, subtropical, and semiarid coastline environments (Devaney et al., 2020) . Mangrove habitats are typically characterized by high salinity, tidal influence, strong winds, high temperature, and muddy anoxic soil (Wang et al., 2022). Several species co-exist in the mangrove environment and have different strategies to cope with such stressful conditions (Esteban et al., 2013). Moreover, mangrove forests are among the most carbon-rich ecosystems on Earth, storing vast amounts of soil carbon, which is crucial for the global carbon cycle and alleviating climate changes (Atwood et al., 2017) . Globally, mangrove communities are experiencing a change in soil salinity variation amplitude and flood depths due to sea-level rise and climate change. These conditions may impact mangrove seedlings' morphology and physiology, including growth, abundance, and distribution of this species composition (Wang et al., 2022).

Mangroves have intraspecific population variability in tolerance to abiotic stressors. The adaptations to flooding and salinity are the most critical factors that drive the local distribution of mangrove species (Méndez-alonzo et al., 2016) . Mangrove plants are well-adapted to salt concentrations that exceed the tolerated by most other plant species (Reef and Lovelock, 2015) . Several plant species co-exist in this environment and display different strategies to cope with salinity. The salt tolerance in mangroves ranges from functional obligate halophytes, which achieve their maximum growth at salinities from 5 to 25 ppt, to facultative halophytes and glycophytes, which optimize their growth in freshwater (Méndez-alonzo et al., 2016; Reef and Lovelock, 2015) . However, the literature has contradictory views regarding the obligated or facultative halophyte behaviour in mangroves (Adame et al., 2021; Cheeseman, 2015; Wang et al., 2011) .

Saline environments have a very negative water potential, making water absorption unfavourable. Consequently, the plant's ability to maintain water uptake in saline conditions is key to salt tolerance. Another physiological challenge to salinity exposure is ion toxicity (i.e. Na^+), as a high concentration is potentially cytotoxic to all plants, including mangroves (Reef and Lovelock, 2015) . Mangrove plants have evolved mechanisms to exclude, secrete and accumulate ions, such as the ultrafiltration of salt in the roots, the presence of salt glands, the hyper-accumulation of ions in the vacuoles, and the production of compatible solutes to osmotic adjustment (Esteban et al., 2013; Méndez-alonzo et al., 2016) .

In addition to salinity, mangroves are exposed to harmful stressors such as high light. Under these combined conditions, low stomatal conductance restricting photosynthesis can severely affect plant growth. The osmotic component of salinity decreases soil water potential, promoting stomatal closure and decreasing CO_2 supply for carboxylation in the chloroplasts (Cerqueira et al., 2019) . Secondly, the excessive ion accumulation decreases the efficiency of the Calvin-Benson-Bassham cycle reactions, leading to an imbalance between the production and consumption of the reducing equivalents produced by the photochemical reactions (Lima Neto et al., 2017) . Therefore, plants exposed to these conditions, commonly found in mangrove ecosystems, are prone to excess excitation energy accumulation in chloroplasts and photoinhibition.

The excess excitation energy in chloroplasts increases the production of reactive oxygen species (ROS) and induces oxidative stress. Thus, high salinity impairs photosynthesis by stomatal and metabolic limitations (Souza et al., 2019) . The increased concentration of ROS, produced by the excess excitation energy in chloroplasts, promotes photoinhibition on both photosystems (PSII and PSI) (Lima Neto et al., 2017) . Plants have evolved diverse photoprotective mechanisms to avoid the harmful effects of excess excitation energy and photoinhibition. Strategies to control the light interception by leaves are ubiquitous in plants, and these strategies can be achieved through different processes, such as changes in leaf orientation, leaf rolling, chloroplasts movements, and the presence of reflective structures such as wax, hairs, or salt crystals (Esteban et al., 2013) . In addition, plants have evolved different mechanisms to dissipate the excess excitation energy, such as non-photochemical quenching (NPQ), photorespiration (P_R), cyclic electron flow (CEF), and the water-water cycle (WWC). Moreover, the non-enzymatic and enzymatic antioxidants are crucial to maintaining cell redox homeostasis and scavenging excessive ROS (Cerqueira et al., 2019; Lima Neto et al., 2017; Ziotti et al., 2019) . However, little is known regarding the modulation of photoprotective mechanisms in mangrove species.

We hypothesized that the regulation of the photochemical yield and the antioxidant metabolism are essential to the growth of *Rhizophora mangle* in a saline gradient. We investigated the role of the modulation of PSII quantum yield and the antioxidant metabolism in *R. mangle* to salt tolerance. Biometric parameters, PSII quantum yields, and the antioxidative metabolism of *R. mangle* were evaluated in a salinity gradient. Knowledge of mangrove physiology and tolerance mechanisms to abiotic factors are crucial to conserving and reforestation efforts.

2 Material and Methods

2.1 Plant material and growth conditions

Mature, fresh propagules of *R. mangle* were collected from nearby trees in Cubatão Estuary (Cubatão, São Paulo, Brazil) and sorted by size and weight. Similar propagules were directly planted into pots (20 L) containing commercial substrate (Plantmax PXHA, Eucatex, SP, Brazil) and maintained in a growth chamber with controlled conditions [photosynthetic photon flux density (PPFD) of 400 µmol m^{-2} s^{-1}, temperature of 30ºC/26ºC day/night, relative humidity of ~65% and a 12 h photoperiod]. These controlled conditions mimicked a typical day in the Coastal region of Cubatão, São Paulo, Brazil (23º88'45" S, 46º42'09" W). Plants were cultivated under these conditions for 120 days and watered every two days with distilled water until pot saturation. Three times a week, the pots were supplemented with NaCl solution (10 ppt), and the electrical conductivity was measured to ensure the saline concentration in the substrate. This reference solution was set according to the salinity of the native environment where the propagules were harvested.

After the 120 days growth period, as described above, the plants were separated into four salinity groups: 0, 10, 35, and 70 ppt. These salinity levels are approximately equivalent of 0, 17.02, 53.07 and 96.91 mS/cm, at 25ºC, respectively or approximately 0, 171.11, 598.9 and 1197.8 mM NaCl, respectively. Plants were irrigated daily with their respective saline solutions. Weekly, the pots were abundantly rinsed with freshwater until drained to avoid salt over-accumulation in the substrate. The electrolyte leakage of the drained was measured weekly to maintain the substrate's salt concentration near the respective treatment concentration. Plants were grown under these conditions for 45 days (the time when plants exposed to 70 ppt presented loss of leaf turgor and chlorosis). Five plants were used for each treatment, and an experimental unit was represented by one plant in a 20 L^{-1} plastic pot.

2.2 Chlorophyll a fluorescence analysis

Chlorophyll *a* fluorescence was measured using the saturation pulse method with a portable chlorophyll fluorometer (JR-PAMIII WALZ, Effeltrich, Germany). Leaves were dark-adapted for 30 min for assessing Fo and Fm. Then, the leaves were exposed to actinic light (500 µmol m^{-2} s^{-1}) for at least 30 min to reach a photosynthetic steady state. The actinic light used was near the saturation point observed from previous light curves performed in our lab and close to the cabinet light intensity. The intensity and duration of the saturation

pulses were 8,000 μmol m^{-2} s^{-1} and 0.7 s, respectively. The following parameters were assessed: the potential quantum yield of PSII [Fv/Fm = (Fm-Fo)/Fm]; the effective quantum yield of PSII [YII = (Fm'- Fs)/Fm'], the proportion of opened (qL) and closed (1-qL) PSII states, the non-photochemical quenching [NPQ = (Fm – Fm')/Fm'], the quantum yield of non-regulated non-photochemical energy loss in PSII [Y(NO) = F/Fm] and the quantum yield of regulated non-photochemical energy loss in PSII [Y(NPQ) = F/Fm' - F/Fm]. Fm and Fo are the maximum and minimum fluorescence of dark-adapted leaves, respectively; Fm′ and Fs are the maximum and the steady state, respectively, fluorescence in the light-adapted samples (Klughammer and Schreiber, 2008; Murchie and Lawson, 2013).

2.3 Growth, biomass partition, relative water content, and water potential

Plants were evaluated for stem diameter at 2 cm from the soil with a pachymeter, the number of leaves, and plant height at the end of the experiment. The third expanded leaf, used for photosynthesis measurements, was photographed, and the leaf area was estimated using the software ImageJ (Schneider et al., 2012) . After the *in vivo* biometric measurements, the plants were harvested and separated into aboveground and roots, which were immediately weighed for fresh matter (FM).

The relative water content (RWC) was calculated from the fresh, turgid, and dry weights of leaves and roots (Lobo et al., 2015) . The dry matter (DM) was determined after 48 h in an oven at 75 °C, and the turgid weight was measured after six hours of saturation in deionized water at 7 °C in dark-condition. The leaf midday water potential (Ψw) was evaluated using a pressure chamber (3000 Scholander PWSC, ICT International, Armidale, AUS) (Scholander, 1960).

2.4 Membrane damage, lipid peroxidation, pigment contents, Na^+ and K^+ contents

The membrane damage, an indicator of cell integrity, was measured as described previously (Cerqueira et al., 2019) . Segments were placed in tubes containing 10 mL of deionized water and incubated in a shaking water bath for 24 h. After that, the electric conductivity of the medium was measured (L1). Then, the segments were boiled at 95^{o}C for 1h, cooled down to ambient temperature in an ice bath, and measured the electric conductivity (L2). The membrane damage (MD) was calculated as MD = (L1/L2) x 100 and expressed in %. The lipid peroxidation was assessed based on the formation of thiobarbituric acid-reactive substances (TBARS) (Cakmak and Horst, 1991) . The TBARS

concentration was calculated using the absorption coefficient (155 mM^{-1} cm^{-1}) and expressed as nmol MDA-TBA g^{-1} FM.

Chlorophyll a, b, total, and carotenoids were measured according to Lichtenthaler and Wellburn, 1983. Leaf samples were extracted in 80% cold acetone overnight at 7ºC in dark-condition. After that, the samples were centrifuged at 10,000 rcf for 5 minutes. The supernatant was read in a spectrophotometer at different wavelengths as previously described (Lichtenthaler et al., 1983) . The total anthocyanin content was determined as previously described by (Neff and Chory, 1998) . Leaf segments were extracted in methanol and 1% HCl at 4ºC overnight. After that, chloroform was added to the homogenate and centrifuged at 14,000 rcf for 5 min. The upper fraction was used for spectrophotometric reading at 530 and 657 nm. The total anthocyanins content was expressed as A530-A657 g^{-1} FW. Na^+ and K^+ contents were measured by flame photometry (Lima Neto et al., 2014) .

2.5 H_2O_2 content and enzymatic activities

The H_2O_2 content was measured by the Amplex Red Hydrogen Peroxide/Peroxidase Assay Kit (Invitrogen). Leaf segments were ground in K-phosphate buffer 100 mM (pH 7.5). The crude extract was centrifuged at 12,000 rcf for 30 min at 4 °C. According to the manufacturer protocol, the supernatant was supplemented with 10 mM Amplex-Red and 10 U of horseradish peroxidase. The resorufin production was measured at 560 nm in a spectrophotometer (Zhou et al., 1997) .

The enzymatic activities were assessed from a protein extract. Leaf segments were ground to a fine powder in liquid nitrogen and then extracted in 100 mM Tris-HCl buffer (pH 8.0) containing 30 mM DTT, 20% glycerol, 1 mM ascorbate, and 3% PEG-6000 (Lima Neto et al., 2017b) . The samples were centrifuged at 14,000 rcf for 20 minutes and stored at -20ºC for enzymatic activity determination. The protein content was measured by the Bradford method (Bradford, 1976) using bovine serum albumin as standard.

Total ascorbate peroxidase (APX) activity (EC. 1.11.1.11) was measured following the ascorbate oxidation at 290 nm. The activity was assayed in a reaction mixture containing 0.5 mM ascorbate and 0.1 mM EDTA dissolved in 100 mM K-phosphate buffer (pH 7.0) and the enzyme extract. The reaction was started by adding 30 mM H_2O_2. The enzymatic activity was measured following the decrease in absorbance at 290 nm and 25 °C, over 300 s, and expressed as µmol ascorbate mg^{-1} protein min^{-1} (Nakano and Asada, 1981) . Total superoxide dismutase (SOD) activity (EC 1.15.1.1) was determined by measuring the

196 inhibition of the blue formazan production by the nitroblue tetrazolium chloride (NBT)
197 photoreduction. SOD activity was measured by adding the leaf extract to a mixture
198 containing 50 mM potassium phosphate buffer (pH 7.8), 0.1 mM EDTA, 13 mM L-
199 methionine, 2 µM riboflavin, and 75 µM p-NBT in the dark. The reaction was carried out
200 under illumination (30 W fluorescent lamp) at 25 °C for 6 min. The absorbance was
201 measured at 540 nm (Giannopolotis and Ries, 1977) . One unit of SOD activity was defined
202 as the amount of enzyme required to inhibit 50% of the NBT photoreduction, and activity
203 was expressed as U mg protein min^{-1}. Total catalase (CAT) activity (EC 1.11.1.6) was
204 measured following the oxidation of H_2O_2 at 240 nm. CAT activity was determined by the
205 reaction of the crude enzyme extract in 50 mM potassium phosphate buffer (pH 7.0)
206 containing 20 mM H_2O_2. The absorbance at 240 nm was measured over 300 s (Havir and
207 McHale, 1987) , and CAT activity was calculated according to the molar extinction
208 coefficient of H_2O_2 (36 mM cm^{-1}) and expressed as µmol H_2O_2 mg^{-1} protein min^{-1}.

209 *2.6 Correlation-based network analysis*

210 Correlation-based networks, including all physiological traits, were calculated using
211 Pearson's product-moment correlation for each of the matrices of data from *R. mangle* under
212 the four treatments (0, 10, 35, and 70 ppt). The nodes correspond to the physiological and
213 biochemical evaluated parameters, and the links correspond to the strength of the
214 connection between the nodes (in module) by Pearson correlation. Networks were designed
215 by restricting the strength of the connections to a specific limit of Pearson correlation
216 coefficient [(r) (-0,80 > r > 0,80)]. The parameters calculated from the networks were
217 obtained as described by Assenov et al. (2008) . Correlation analyses were performed by
218 Pearson correlation using the Correlation Calculator software (Basu et al., 2017) , and
219 weighted correlation-based scale-free networks were calculated using MetScape 3 on
220 Cytoscape v. 3.9.1.

221 *2.7 Statistical analysis*

222 The experiment was arranged in a completely randomized design, with four treatments
223 (0, 10, 35, and 70 ppt NaCl) containing five replicates represented by one plant per pot. All
224 dependent variables were analyzed by one-way *ANOVA* and the means were compared by
225 Tukey's test ($P \leq 0.05$). Box plots show medians and first and third quartiles (25th and 75th
226 percentiles), and whiskers extend from the hinge to the largest or smallest value, no further
227 than 1.5 times. The statistical analyses shown in the plots were performed using R (version
228 4.0.2) and Rstudio version (1.3.959). Multivariate principal component analysis (*PCA*) was

performed on all analyzed dependents. Before *PCA* analysis, data were scaled to reduce the effect of different variables, allowing data standardization. The level of importance of each PC was determined by the broken-stick method (Vítolo et al., 2012) . The PCA was performed using the RFactoMineR and factoextra packages in R.

3 Results

3.1 Hypersalinity reduced growth, water status, $[K^+]/[Na^+]$ ratio and increased membrane damage in Rhizophora mangle

The total fresh plant biomass did not change in plants exposed to 0, 10, and 35 ppt. However, it was significantly decreased by 28% in plants exposed 70 ppt (hypersalinity) compared with plants grown under 10 ppt (the salinity of the environment where the plants were collected, called in this research as control) (Figure 1). Hypersalinity also negatively impacted the biomass partition compared to plants submitted to 10 ppt (control) (Figure 1). Plants grown in freshwater (~0 ppt) did not show significant differences in biomass allocation compared with plants grown under 10 ppt (Figure 1). Biometric parameters such as plant height, leaf area, and the number of leaves were also decreased by 35 ppt and hypersalinity (70 ppt), except the stem diameter, which was significantly increased compared to the control plants (plants grown in 10 ppt) (Table 1). However, these parameters did not change in plants grown in freshwater (~0 ppt) compared with the reference plants (10 ppt) (Table 1).

The relative water content (RWC) and membrane damage (MD) in leaves and roots were strongly affected by salinity (Figure 2). The RWC was decreased by 38% in leaves and 15% in roots, while MD significantly increased in both plant organs (~3-fold) in plants exposed to 70 ppt, compared to plants grown in 10 ppt (Figure 2). Freshwater (~0 ppt) significantly decreased the leaf RWC in leaves, but this parameter did not change in roots compared to the reference plants (10 ppt) (Figure 2 A-B). The membrane damage (MD) also increased in leaves and roots of plants grown in freshwater (~0 ppt) compared to control plants (10 ppt) (Figure 2 C-D).

The leaf water potential was significantly decreased by 65% in plants exposed to 70 ppt compared with control plants (10 ppt) (Figure 3A). In contrast, plants cultivated in freshwater (~0 ppt) did not change their water potential compared to control (Figure 3A). The leaf succulence presented the lowest value in plants grown in freshwater and the highest value in plants grown in 35 ppt. Moreover, the leaf succulence was not affected by hypersalinity (70 ppt) compared with control (Fig 3B). The $[K^+]/[Na^+]$ ratio significantly

increased in leaves and roots (2- and 6-fold, respectively) of plants grown in ~0 ppt. This ratio significantly decreased in leaves and roots of plants submitted to 35 and 70 ppt, all compared with control (Figure 3C-D). As expected, the $[K^+]/[Na^+]$ ratio significantly decreased as the salinity increased in a dose-response trend.

3.2 Photosynthetic pigment contents and PSII activity were severely affected by hypersalinity

The total chlorophyll content (*TCC*) was significantly reduced in plants exposed to 70 ppt, whereas it did not change in plants grown in freshwater compared to the reference plants (10 ppt). This parameter was lower in plants grown under 35 ppt than in the reference plants, and it did not change when compared to 70 ppt (Table 2). The chlorophyll a/b ratio significantly decreased in plants exposed to 35 ppt and *70 ppt* compared to the reference plants. In contrast, this ratio did not change in plants grown in freshwater compared to plants grown in 10 ppt (Table 2). The carotenoid content decreased by 39% in freshwater, and increased by 27% in 70 ppt compared with the control plants, respectively (Table 2). The anthocyanin content significantly increased by ~2-fold in plants exposed to 70 ppt, but did not change in freshwater plants compared with the reference plants (Table 2). These pigment changes contributed to modifications in PSII performance, especially in plants grown in hypersalinity, as described below.

The potential quantum yield of PSII (*Fv/Fm*) was not significantly affected in plants grown in different salinity conditions. This pattern shows that the plants were not photoinhibited (Figure 4A). The effective quantum yield of PSII [*Y(II)*] significantly reduced in plants exposed to 35 and 70 ppt. In contrast, *YII* was not affected by freshwater compared to the reference plants (Figure 4B). The open centers of PSII (*qL*) were only changed in plants exposed to 35 and 70, compared with the reference plants (10 ppt) (Figure 4C). In contrast, the non-photochemical quenching (NPQ) related parameters were enhanced by 35 and 70 ppt, respectively (Figure 5). The PSII closed centers (*1-qL*) and the NPQ increased in 35 and 70 ppt plants compared with reference plants (Figure 5A-B). The freshwater did not change these parameters compared to the reference plants (Figure 5A-B). The non-regulated non-photochemical energy loss of PSIII [*Y(NO)*] was higher in plants grown at 35 and 70 ppt than in the reference plants (10 ppt). This parameter did not change in plants submitted to freshwater compared with the reference plants (Figure 5C). Besides the *NPQ* did not change in plants grown in 35 ppt compared to 70 ppt, the non-regulated *NPQ (YNO)* was higher in plants under 70 ppt compared to plants grown in 35 ppt. In

contrast, the regulated portion of the *NPQ* [*Y(NPQ)*] significantly increased in plants grown in 35 ppt than in plants exposed to 70 ppt.

3.3 Oxidative stress indicators and antioxidant enzyme activities showed different patterns in response to freshwater and hypersalinity

To evaluate the aspects of the modulation of PSII quantum yields to photoprotection and the avoidance of ROS accumulation and oxidative stress, we evaluated lipid peroxidation, hydrogen peroxide content, and three major antioxidant enzyme activities. The lipid peroxidation, assessed by the thiobarbituric acid reactive substances (TBARS), increased as the salinity concentration became higher (Table 3). The H_2O_2 content in leaves followed the same trend as TBARS (Table 3). The superoxide dismutase (SOD) and catalase activities in leaves of *R. mangle* presented higher values as the NaCl concentration increased (Table 3). Plants grown in freshwater showed lower SOD, CAT, and ascorbate peroxidase (APX) activities than the reference plants (Table 3). The APX activity was lower in plants exposed to 70 ppt than in the reference plants and plants cultivated in 35 ppt (Table 3).

3.4 Systemic view of physiological indicators in R. mangle to different salinity

We performed a multivariate principal component analysis to summarize the information based on the many variables assessed and better understand the data set variation. The distribution of the variables determined in this study, including all treatments, is shown in Supplemental figure 1. PCA 1 and PCA 2 explained 80.6% of the total variance (Supplemental figure 1). The Na^+ content in leaves, anthocyanin concentration, YNO, H_2O_2 content, and Na^+ in roots were the main relevant variables for principal components 1 and 2. In contrast, Fv/Fm, total fresh matter, and leaf succulence were the less relevant variables for PC1 and PC2 (Supplemental figure 1). Additionally, the K^+ content in roots and leaves and the relative water content in roots showed a distinct behaviour compared with other variables, as essential components only in plants exposed to freshwater (0 ppt) (Supplemental figure 1). There was a clear distribution pattern among treatments, with each treatment separated into a distinct quadrant (Supplemental figure 1).

The weighted correlation-based network analysis (WCNA) presented well-defined differences in plants exposed to freshwater and 10 ppt, compared with plants grown under 35 and 70 ppt (Supplemental figure 2). Plants grown under freshwater or 10 ppt presented more loosened networks than plants under 35 and 70 ppt. Moreover, plants under 70 ppt

showed the highest network centralization (Supplemental table 1). Control plants grown in 10 ppt showed the highest number of nodes, edges, average number of neighbours, clustering coefficient, and network density (Supplemental table 1). In contrast, the network parameters from plants grown under 35 ppt showed the lowest values of the number of edges, average number of neighbours, clustering coefficient, network density, heterogeneity, and centralization (Supplemental table 1).

4 Discussion

4.1 Rhizophora mangle showed similar growth in freshwater and low salinity, but it was severely affected by hypersalinity, a common pattern of facultative halophytes

Although *R. mangle* is commonly considered a halophyte species, there are contradictory views regarding the relationship between mangroves and salt stress in the literature (Wang et al., 2011) . Some authors argue that mangroves are considered facultative halophytes, as freshwater is a physiological requirement while saltwater is an ecological requirement (Krauss and Ball, 2013) . This latter condition prevents the invasion and competition with non-halophyte plants for the restricted resources in the mangrove environment. In contrast, some reports describe mangroves as obligate halophytes, which cannot grow in permanent freshwater; consequently, salt is a physiological requirement (Lugo and Snedaker, 1974) . Nevertheless, *R. mangle* plants are sensitive to hypersalinity. It is important to note that there is no consensus in the literature regarding mangrove's hypersalinity threshold. However, according to Devaney et al. (2020) , hypersaline conditions range from salt concentrations above 50 ppt, which corroborates with the salinities used in this research as hypersalinity (70 ppt).

In our study, *R. mangle* exposed to hypersalinity showed lower plant height, less biomass accumulation and leaf area, and a lower number of leaves compared with plants grown in a saline concentration equivalent to their natural environment (10 ppt) or compared to plants grown in freshwater (Table 1 and Figure 1). In opposition, the stem diameter was significantly increased in plants exposed to hypersalinity (Table 1). These parameters were not affected in plants cultivated in freshwater (0 ppt) compared with plants exposed to 10 ppt. Growth performance is a sensitive indicator of tolerance in plants exposed to salinity. Non-halophytes survive optimally in freshwater and mortality is imminent at slightly higher salinity concentrations. Facultative halophytes can also grow in freshwater but differ from non-halophytes in responding to increases in salinity with promoted growth, up to an optimum level, above which growth would decrease. Finally, obligate halophytes have

optimal growth under ranges of salinity similar or greater to those of facultative halophytes but differ in their inability to survive under freshwater (Cheeseman, 2015; Flowers and Colmer, 2015, 2008; Krauss and Ball, 2013; Wang and Yan, 2011) . Therefore, it suggests that *R. mangle* is a facultative halophyte, as it can survive in freshwater, even though its growth was slightly reduced.

4.2 Osmotic protection and ion partitioning maintain an optimum water status and cellular integrity under hypersalinity in R. mangle

R. mangle plants can grow and flower regularly when irrigated with freshwater (Wang and Yan, 2011; Werner and Stelzer, 1990) . Plants grown in 35 ppt or 70 ppt showed significant alterations in biometric parameters (Figure 1 and Table 1). These biometric alterations induced by 35 ppt and 70 ppt are related to the reduced leaf water potential and the relative imbalance in the $[K^+]/[Na^+]$ ratio in leaves and roots (Figure 3). It was previously shown that *R. mangle* could keep extremely low leaf water potentials (-5 MPa), maintaining their hydraulic system safe (Méndez-alonzo et al., 2016) . Hence, the higher stem diameter in plants exposed to 35 and 70 ppt could be related to a better hydraulic conductivity efficiency in low water potential (Méndez-alonzo et al., 2016).

Maintaining an efficient stem hydraulic system is important to ensure the hydraulic conductivity of leaves under low water potential, sustaining transpiration and photosynthesis. Mangroves typically have relatively low transpiration rates and high water use efficiencies (Lovelock et al., 2006) . Lower stomatal conductance resulting from increasing substrate salinity in mangroves is well established; when soil salinity is greater than the seawater salt concentration (35 ppt), the whole-plant hydraulic conductance can decline due to xylem cavitation, resulting in severe limitations of photosynthesis and growth (Méndez-alonzo et al., 2016) , which is in accordance with our data. *R. mangle* leaves also showed higher water content per unit area (leaf succulence) under salinity conditions than in plants cultivated in freshwater (0 ppt) (Fig. 3). This response corroborates with previous research, suggesting that leaf succulence increases as salinity rises (Camilleri and Ribi, 1983) .

Mangroves have relatively low photosynthetic carbon gain and reduced productivity. Decreased number of leaves, leaf area, and height could be energetically efficient in this species under salt stress (Munns et al., 2020) . As an osmotic effect of the salt stress, the stomatal closing decreases leaf transpiration, water intake, and, consequently, salt intake. This physiological response of tolerant species avoids the toxic effects of the excess Na^+

concentration in the leaf tissue (Flowers and Colmer, 2008). However, the CO_2 assimilation is decreased by stomatal limitation, consequently promoting the excess excitation energy in the chloroplasts, as the Calvin-Benson-Bassham cycle reactions are the main sink of the reducing equivalents produced by the photochemical reactions (Cerqueira et al., 2019). Thus, increases in the water content in leaves exposed to salinity (salt succulence) enhance the leaf's capacity to dissipate heat, reducing the need for evaporative cooling. This is an important mechanism in plants under stomatal closing as *R. mangle* under hypersalinity (Calzadilla et al., 2022).

Like many other halophytes, mangroves use the accumulation of select ions as solutes to adjust the osmotic potential (Reef and Lovelock, 2015), which is in accordance with our data (Figure 3). However, in mangroves growing at high salinity, the predicted shoot osmotic potential, calculated from cellular ion concentrations, is higher than the observed one (Méndez-alonzo et al., 2016). Therefore, above the hypersalinity threshold, other compatible osmotic substances are necessary to reduce the water potential and maintain water uptake. The membrane damage, an indicator of cell integrity, was increased in plants exposed to hypersalinity and slightly increased in plants cultivated in freshwater compared with reference plants (Figure 2), corroborating the importance of osmotic adjustment to cell integrity.

Low salinity maintained cell integrity in *R. mangle* compared with plants cultivated in 0, 35, and 70 ppt (Figure 2). Probably, low salinity was able to induce osmotic protection by the accumulation of compatible solutes, which could promote cell organelles protection and whole-cell integrity. However, little is known regarding the metabolism of the accumulation of organic compatible solutes to salt acclimated-*R. mangle* and its influence on salt acclimation (Munns et al., 2020). *R. mangle* plants cultivated in freshwater showed a significant Na^+ concentration in leaves and roots (Figure 3). This could be explained as viviparous mangroves, as *R. mangle* have larger propagules that store large amounts of nutrients and energy (Yan et al., 2007) and high concentrations of Na^+ and Cl^- (Wang and Yan, 2011). Thus, even growing in freshwater in the short term, *Rhizophora* seedlings still have significant concentrations of Na^+ and Cl^-.

4.3 The plasticity and resilience of the photosynthetic apparatus of R. mangle under salinity

The modulation of the photosynthetic PSII quantum yields was evaluated by chlorophyll *a* fluorescence analysis. The potential quantum yield of photosystem II (PSII) (Fv/Fm), an indicator of the maximum photosynthetic yield, did not change in plants exposed

to hypersalinity or the absence of NaCl compared to the reference plants (Figure 4). Roughly, high Fv/Fm could indicate that PSII is not photoinhibited. However, to avoid photoinhibition, this species should modulate the use and efficiency of the different quantum yields of both photosystems (Lima Neto et al., 2017b).

Under photoinhibited conditions, $P680^{+}$ lifetime increases, and this powerful oxidant may degrade pigments and amino acids nearby. On the other hand, when the acceptor side is less efficient, a P680 triplet radical is formed, interacting with atmospheric oxygen (O_2), forming singlet oxygen ($^1O_2$). These reactive oxygen species degrade D1 protein in the core of the PSII reaction center (Lima Neto et al., 2017b). As a response to hypersalinity, *R. mangle* plants significantly decreased the effective quantum yield of PSII [Y(II)] compared with plants exposed to the reference treatment and freshwater (Fig. 4). Also, plants under hypersalinity displayed a higher portion of reduced Qa, indicated by the decrease in qL, showing a closed state of PSII by an acceptor site limitation (Cerqueira et al., 2019). Hence, the decrease in Y(II) by plants exposed to hypersalinity was followed by the increase in the closed state of Qa (1-qL) (Figure 5), indicating an acceptor site limitation of PSII. Denvaney et al. (2020) showed that Y(II) changes in *R. mangle* were not significantly related to soil salinity. However, where soils were hypersaline (ranging from 55 to 78 ppt), the Y(II) strongly decreased as soil salinity enhanced. Also, at soil salinities >60 ppt, Y(II), growth and the survival of *R. mangle* seedlings were severely reduced (Devaney et al., 2020), which is in accordance with our data. Previous works have demonstrated that photoinhibition occurs in hypersaline conditions for several species (Biber, 2006; Naidoo, 2006; Sobrado, 2000).

R. mangle exposed to hypersalinity strongly induced the dissipation of excess excitation energy by the non-photochemical quenching (NPQ) (Figure 5). This mechanism protects the reaction centers of PSII via rapid dissipation of excess excitation energy as heat. It is essential to mention that the PSII quantum yield efficiency can be decreased by damaging the PSII reaction center or inducing NPQ (Areington et al., 2022). The contribution of these aspects to the NPQ increase was estimated by the evaluation of the quantum yield of the non-regulated [Y(NO)] and regulated [Y(NPQ)] non-photochemical energy losses in PSII. It was shown that the regulated NPQ portion was the relatively most crucial component of the increase in NPQ in *R. mangle* exposed to hypersalinity (Figures 5C-D).

Corroborating these previous results, the carotenoid and anthocyanin contents, both pigments involved in photoprotection, were increased in *R. mangle* exposed to 70 ppt (Table 2). Moreover, the chlorophyll contents were decreased in plants exposed to 70 ppt, probably

458 to reduce light-harvesting and consequently excess excitation energy in the chloroplasts.
459 Even with the decrease in chlorophyll content, plants exposed to hypersalinity tended to
460 present a lower chlorophyll a/b ratio, which may be involved with a photoprotection
461 mechanism to avoid light-harvesting and, consequently, excess excitation energy in
462 chloroplasts (Lima Neto et al., 2017b).

463 *4.4 The dissipation of excess excitation energy in chloroplasts was not able to avoid*
464 *oxidative stress in R. mangle exposed to hypersalinity*

465 The lipid peroxidation and H_2O_2 were increased due to the increased NaCl
466 concentration (Table 3). The over-reduction of the electron transport chain in mitochondria
467 and chloroplasts are the main sites of ROS production. Plants have evolved different
468 metabolic strategies to scavenge excess ROS. In particular, ROS is involved with signalling
469 processes, but the excess constantly challenges the chloroplast during photochemical
470 reactions. The disruption of the balance between the photochemical reactions, producing
471 the reducing equivalents and their consumption by the Calvin-Benson-Bassham cycle, is a
472 prominent situation of ROS production, promoting photoinhibition (Lima Neto et al., 2017b).
473 Thus, the balance between ROS production and their removal by enzymatic and non-
474 enzymatic antioxidants determines the type and concentration of ROS present and to what
475 extent damage will occur (Foyer et al., 2017).

476 *R. mangle* plants exposed to elevated salt concentrations increased the SOD and CAT
477 activities in leaves (Table 3). These enzymes work in a synchronized way, forming an
478 efficient antioxidant system. The SOD will catalyze the scavenging of the superoxide radical,
479 forming H_2O_2 which is further removed by CAT. Thus, in our data, the activities of these
480 enzymes are positively correlated and work together to remove the excess ROS produced
481 by the effects of high salinity. On the other hand, the APX activity was higher in the reference
482 plants, and its activity was decreased in plants exposed to freshwater and hypersalinity
483 (Table 3). It was previously shown that salt enhanced SOD activity, which was not matched
484 by APX activity (Gueta-Dahan et al., 1997). Moreover, these authors suggest that APX is a
485 salt-sensitive enzyme, inhibited by the excess of H_2O_2 (Moschetto et al., 2019). Thus, in our
486 study, the increase in the H_2O_2 content produced by hypersalinity probably impaired the
487 activity of APX in *R. mangle*.

488 *4.5 Physiological network plasticity promotes tolerance to different ranges of salinity in*
489 *Rhizophora mangle*

The responses of plants to environmental complexity are the sum of their modular responses and all the interaction effects resulting from the integration of individual modules, which allows emergent properties of biological systems (Souza and Lüttge, 2015). Thus, no single scale can represent whole-plant plasticity (Bertolli et al., 2013; Vítolo et al., 2012). The functional plasticity in *R. mangle* plants is given by multifunctional regulatory capacity, permitting performance variations in different saline conditions. It is based on network structures and topology providing high degrees of flexibility (Supplemental Table 1 and Supplemental Figure 1).

Our data clearly show that plants exposed to different saline levels could adjust different morphometric and physiological responses to acclimation (Supplemental Figures 1 and 2). Plants exposed to freshwater or low salinity (10 ppt) presented more approximated network topologies when compared with plants exposed to 35 and 70 ppt (Supplemental Figure 2 and Supplemental Table 1). These data show a systemic view of the acclimation responses of *R. mangle* as an integrated response with the interaction and flux of energy and information among different modules and physiological responses.

5. Conclusions

This study demonstrates that saline acclimation and tolerance of *Rhizophora mangle* is a complex phenomenon influenced by an integrated variety of metabolic and physiological responses. *R. mangle* plants can grow and develop in the presence of freshwater (absence of salt) and moderate salinity. In contrast, under hypersaline conditions, growth and biomass accumulation is impaired. In response to hypersalinity, the biomass partition and the accumulation of ions and compatible solutes are modulated to maintain the water status. Moreover, the plasticity in the efficiency of the quantum yields on PSII is crucial to dissipate the excess excitation energy avoiding photoinhibition in *R. mangle* exposed to hypersalinity.

Plants grown under constant salinity in a laboratory setting are unlikely to behave similarly to those in their natural habitat with fluctuating salinity. Thus, studies on the effects of freshwater, low salinity, and salinity fluctuation on mangroves and the physiological mechanisms under fluctuating salinity conditions should be strengthened in future research.

Authors contribution section

BPS, **HMS,** and **YB**: investigation, validation, formal analysis. **AKML**: formal analysis, review & editing, visualization. **MCLN**: conceptualization, methodology, resources, writing original draft, review & editing, supervision, funding acquisition, and project administration.

Declaration of competing interest

The authors declare that they have no competing financial interests or personal relationships that could have appeared to influence the work reported in this paper.

Acknowledgments/Funding

The authors would like to thank the financial support from grants #2019/26850-7 AKML, #201919245-0 HMS and #2018/04258-6 MCLN, São Paulo Research Foundation (FAPESP) and grant #404707/2018-1, National Council for Scientific and Technological Development CNPq, MCLN.

Figure Captions

Figure 1- Biomass partition (aboveground and root) of *Rhizophora mangle* exposed to 0, 10, 35 and 70 ppt NaCl in a growth chamber. Data represent the means (bars and numbers in white) and standard deviation of five biological replicates. According to Tukey's test, different letters represent significant differences between treatments ($P \leq 0.05$).

Figure 2 - Leaf (A, C) and root (B, D) relative water content and membrane damage of *Rhizophora mangle* exposed to 0, 10, 35 and 70 ppt NaCl. Boxes represent the median and first and third quartiles (n = five biological replicates), and whiskers represent the standard deviation. According to Tukey's test, different letters represent significant differences between treatments ($P \leq 0.05$).

Figure 3: Leaf water potential (A) and succulence (B), and the $[K^+]/[Na^+]$ ratio in leaves (C) and roots (D) of *Rhizophora mangle* exposed 0, 10, 35 and 70 ppt NaCl. Boxes represent the median and first and third quartiles (n = five biological replicates) and whiskers represent the standard deviation. According to Tukey's test, different letters represent significant differences between treatments ($P \leq 0.05$).

Figure 4: Potential quantum yield of PSII (A), effective quantum yield of PSII (B), and open PSII centers (D) of leaves of *Rhizophora mangle* exposed to 0, 10, 35 and 70 ppt NaCl. Boxes represent the median and first and third quartiles (n= five biological replicates) and whiskers represent the standard deviation. According to Tukey's test, different letters represent significant differences between treatments ($P \leq 0.05$).

Figure 5: Closed PSII centers (A), non-photochemical quenching (B), quantum yield of non-regulated (C), and regulated (D) non-photochemical energy loss of PSII of leaves of *Rhizophora mangle* exposed to 0, 10, 35 and 70 ppt NaCl. Boxes represent the median and first and third quartiles (n = five biological replicates) and whiskers represent the standard deviation. According to Tukey's test, different letters represent significant differences between treatments ($P \leq 0.05$).

Figure S1: PCA ordination diagram of variables plots with significant variation across salinity levels. The two axes (PCA 1 and 2) explained 80.6% of the variance. The percentage of variation explained by each principal component is shown. Red circles represent plants grown at 70 ppt NaCl. Orange circles represent plants grown at 35 ppt NaCl. Yellow circles represent plants grown at 10 ppt NaCl and green circles, plants grown in freshwater. Variable caption: rwc_leaf is the relative water content in leaves, rwc_root is the relative water content in roots, tfm is the total fresh matter, wpot is the water potential, k_leaf and k_root are the K^+ content in leaves and roots respectively, md_leaf and md_roots are the membrane damage in leaves and roots respectively, car is the carotenoid content in leaves, diameter is the stem diameter, na_leaf and na_root are the Na+ contents in leaves and roots respectively.

Figure S2: Correlation-based networks of physiological parameters in *R. mangle* plants cultivated in freshwater (A), 10 ppt NaCl (B), 35 ppt NaCl (C) and 70 ppt NaCl (D). Nodes represent physiological parameters and lines their pairwise correlations. Blue links represent a positive correlation and red links represent a negative correlation. Ticker links indicate a higher correlation in module (n = 5).

570 **Table 1**: Plant height, stem diameter, leaf area and number of leaves of Rhizophora mangle exposed
571 to salinity levels in a growth chamber. Values represent the mean ± SD of five biological replicates
572 (n = 5). According to Tukey's test, different letters represent significant differences between
573 treatments (P ≤ 0.05)

574

	0	**10**	**35**	**70**
Plant height (cm plant^{-1})	48.84 ± 1.73a	51.85 ± 1.96a	40.42 ±1.08b	36.06 ± 1.52b
Stem diameter (cm plant^{-1})	8.20 ± 0.66b	10.30 ± 0.67b	13.27 ± 0.44a	13.04 ± 0.48a
Leaf area (cm^2)	43.29 ± 2.58a	42.68 ± 2.87ab	33.68 ± 1.27bc	24.78 ± 1.03c
Number of leaves (plant^{-1})	14.00 ± 0.58a	12.33 ± 0.33ab	10.67 ± 0.67b	7.67 ± 0.33c

575

576 **Table 2:** Total chlorophyll content, chlorophyll a/b ratio, carotenoids and anthocyanin contents in
577 leaves of *Rhizophora mangle* exposed to increasing salinity. Values represent the mean ± SD of five
578 biological replicates (n = 5). According to Tukey's test, different letters represent significant
579 differences among treatments (P ≤ 0.05).

	0	**10**	**35**	**70**
Total Chl (mg g^{-1} FM)	99.21 ± 7.75a	94.95 ± 6.97a	67.85 ± 1.50b	56.52 ± 2.62b
Chl a/Chl b ratio	2.40 ± 0.30a	2.00 ± 0.03a	1.38 ± 0.08b	1.53 ± 0.06b
Carotenoids (mg g^{-1} FM)	95.54 ± 3.19c	152.16 ± 9.20b	174.60 ± 4.45b	193.54 ± 4.70a
Anthocyanin (mg g^{-1} FM)	0.98 ± 0.07b	1.19 ± 0.04b	2.01 ± 0.07a	2.28 ± 0.14a

580

581 **Table 3:** Contents of TBARS (lipid peroxidation) and H_2O_2, and the activities of superoxide
582 dismutase, ascorbate peroxidase and catalase in leaves of *Rhizophora mangle* exposed to
583 increasing salinity. Values represent the mean ± SD of five biological replicates (n = 5).
584 According to Tukey's test, different letters represent significant differences among treatments
585 ($P \leq 0.05$).

	0	**10**	**35**	**70**
TBARS content (nmol MDA-TBA g^{-1} FM)	42.91 ± 4.70c	85.39 ± 4.08b	97.40 ± 2.65ab	106.09 ± 3.99a
H_2O_2 content (ηmol g^{-1} FM)	12.04 ± 0.38c	30.74 ± 1.14b	44.53 ± 2.00a	47.12 ± 0.52a
SOD activity (U mg^{-1} protein min^{-1})	2.58 ± 0.40c	3.87 ± 0.38bc	5.55 ± 0.32ab	6.34 ± 0.45a
APX activity (mmol mg^{-1} protein min^{-1})	0.81 ± 0.09c	2.76 ± 0.20b	3.87 ± 0.37a	1.04 ± 0.02c
CAT activity (mmol mg^{-1} protein min^{-1})	95.54 ± 3.19c	152.16 ± 9.20b	174.60 ± 4.45ab	193.54 ± 4.70a

586 **References**

Adame, M.F., Reef, R., Santini, N.S., Najera, E., Turschwell, M.P., Hayes, M.A., Masque, P., Lovelock, C.E., 2021. Mangroves in arid regions: Ecology, threats, and opportunities. Estuarine, Coastal and Shelf Science 248, 106796. https://doi.org/10.1016/j.ecss.2020.106796

Areington, C.A., Lima Neto, M.C., Watt, P.M., Sershen, 2022. Assessing the utility of selected photosynthetic and related traits in screening Amaranthus dubius Mart. ex Thell. and Galinsoga parviflora Cav. 1796 seedlings for elevated temperature stress tolerance. South African Journal of Botany 000. https://doi.org/10.1016/j.sajb.2022.02.037

Assenov, Y., Ramírez, F., Schelhorn, S.E.S.E., Lengauer, T., Albrecht, M., 2008. Computing topological parameters of biological networks. Bioinformatics 24, 282–284. https://doi.org/10.1093/bioinformatics/btm554

Atwood, T.B., Connolly, R.M., Almahasheer, H., Carnell, P.E., Duarte, C.M., Ewers Lewis, C.J., Irigoien, X., Kelleway, J.J., Lavery, P.S., Macreadie, P.I., Serrano, O., Sanders, C.J., Santos, I., Steven, A.D.L., Lovelock, C.E., 2017. Global patterns in mangrove soil carbon stocks and losses. Nature Climate Change 7, 523–528. https://doi.org/10.1038/nclimate3326

Basu, S., Duren, W., Evans, C.R., Burant, C.F., Michailidis, G., Karnovsky, A., 2017. Sparse network modeling and metscape-based visualization methods for the analysis of large-scale metabolomics data. Bioinformatics 33, 1545–1553. https://doi.org/10.1093/bioinformatics/btx012

Bertolli, S.C., Vítolo, H.F., Souza, G.M., 2013. Network connectance analysis as a tool to understand homeostasis of plants under environmental changes. Plants 2, 473–488. https://doi.org/10.3390/plants2030473

Biber, P.D., Biber, P.D., 2006. Measuring the effects of salinity stress in the red mangrove, Rhizophora mangle L. African Journal of Agricultural Research 1, 001–004.

Bradford, M.M., 1976. A rapid and sensitive method for the quantification of microgram quantities of protein utilizing the principle of protein-dye binding. Analytical Biochemistry 722, 248–254.

Cakmak, I., Horst, W.J., 1991. Effect of aluminium on lipid peroxidation, superoxide dismutase, catalase, and peroxidase activities in root tips of soybean (Glycine max). Physiologia Plantarum 83, 463–468. https://doi.org/10.1111/j.1399-3054.1991.tb00121.x

Calzadilla, P.I., Carvalho, F.E.L., Gomez, R., Lima Neto, M.C., Signorelli, S., 2022. Assessing photosynthesis in plant systems: A cornerstone to aid in the selection of resistant and productive crops. Environmental and Experimental Botany 201, 104950. https://doi.org/10.1016/j.envexpbot.2022.104950

Camilleri, J.C., Ribi, G., 1983. Leaf Thickness of Mangroves (Rhizophora mangle) Growing in Different Salinities. Biotropica 15, 139. https://doi.org/10.2307/2387959

Cerqueira, J.V.A., Silveira, J.A.G., Carvalho, F.E.L., Cunha, J.R., Lima Neto, M.C., 2019. The regulation of P700 is an important photoprotective mechanism to NaCl-salinity in Jatropha curcas. Physiologia Plantarum. https://doi.org/10.1111/ppl.12908

Cheeseman, J.M., 2015. The evolution of halophytes, glycophytes and crops, and its implications for food security under saline conditions. New Phytologist 206, 557–570. https://doi.org/10.1111/nph.13217

Devaney, J.L., Marone, D., Mcelwain, J.C., 2020. Impact of soil salinity on mangrove restoration in a semiarid region : a case study from the Saloum Delta , Senegal 29, 1–10. https://doi.org/10.1111/rec.13186

Esteban, R., Fernández-Marín, B., Hernandez, a., Jiménez, E.T., León, a., García-Mauriño, S., Silva, C.D., Dolmus, J.R., Dolmus, C.M., Molina, M.J., Gutierrez, N.N., Loaisiga, M.I., Brito, P., García-Plazaola, J.I., 2013. Salt crystal deposition as a reversible mechanism to enhance photoprotection in black mangrove. Trees - Structure and Function 27, 229–237. https://doi.org/10.1007/s00468-012-0790-8

Flowers, T.J., Colmer, T.D., 2015. Plant salt tolerance: adaptations in halophytes. Annals of Botany 115, 327–331. https://doi.org/10.1093/aob/mcu267

Flowers, T.J., Colmer, T.D., 2008. Salinity tolerance in halophytes. The New phytologist 179, 945–63. https://doi.org/10.1111/j.1469-8137.2008.02531.x

Foyer, C.H., Ruban, A.V., Noctor, G., 2017. Viewing oxidative stress through the lens of oxidative signalling rather than damage. Biochemical Journal 474, 877–883. https://doi.org/10.1042/BCJ20160814

Giannopolotis, C.N., Ries, S.K., 1977. Superoxide dismutases: Occurrence in higher plants. Plant Physiology 59, 309–314.

Gomes Soares, M.L., Pereira Tognella, M.M., Cuevas, E., Medina, E., 2015. Photosynthetic capacity and intrinsic water-use efficiency of Rhizophora mangle at its southernmost western Atlantic range. Photosynthetica 53, 464–470. https://doi.org/10.1007/s11099-015-0119-0

Gueta-Dahan, Y., Yaniv, Z., Zilinskas, B.A., Ben-Hayyim, G., 1997. Salt and oxidative stress: similar and specific responses and their relation to salt tolerance in Citrus. Planta 203, 460–469. https://doi.org/10.1007/s004250050215

Havir, E.A., McHale, N.A., 1987. Biochemical and Developmental Characterization of Multiple Forms of Catalase in Tobacco Leaves. Plant Physiology 84, 450–455. https://doi.org/10.1104/pp.84.2.450

Klughammer, C., Schreiber, U., 2008. Complementary PS II quantum yields calculated from simple fluorescence parameters measured by PAM fluorometry and the Saturation Pulse method. PAM Application Notes 1, 27–35. https://doi.org/citeulike-article-id:6352156

Krauss, K.W., Ball, M.C., 2013. On the halophytic nature of mangroves. Trees 27, 7–11. https://doi.org/10.1007/s00468-012-0767-7

Lichtenthaler, H., Wellburn, A., Lichtentharler, H.K., Welburn, A.R., 1983. Determination of total carotenoids and chlorophylls a and b of leaf extracts in different solvents. Biochemical Society Transactions 11, 591–592. https://doi.org/10.1042/bst0110591

Lima Neto, M.C., Cerqueira, J.V.A., Cunha, J.R., Ribeiro, R.V., Silveira, J.A.G., 2017a. Cyclic electron flow, NPQ and photorespiration are crucial for the establishment of young plants of Ricinus communis and Jatropha curcas exposed to drought. Plant Biology 19, 650–659. https://doi.org/10.1111/plb.12573

Lima Neto, M.C., Lobo, A.K.M., Martins, M.O., Fontenele, A.V., Silveira, J.A.G., 2014. Dissipation of excess photosynthetic energy contributes to salinity tolerance: A comparative study of salt-tolerant Ricinus communis and salt-sensitive Jatropha curcas. Journal of Plant Physiology 171, 23–30. https://doi.org/10.1016/j.jplph.2013.09.002

Lima Neto, M.C., Silveira, J.A.G., Cerqueira, J.V.A., Cunha, J.R., 2017b. Regulation of the photosynthetic electron transport and specific photoprotective mechanisms in Ricinus communis under drought and recovery. Acta Physiologiae Plantarum 39, 183. https://doi.org/10.1007/s11738-017-2483-9

Lobo, A.K.M., de Oliveira Martins, M., Lima Neto, M.C., Machado, E.C., Ribeiro, R.V., Silveira, J.A.G., 2015. Exogenous sucrose supply changes sugar metabolism

and reduces photosynthesis of sugarcane through the down-regulation of Rubisco abundance and activity. Journal of Plant Physiology 179, 113–121. https://doi.org/10.1016/j.jplph.2015.03.007

Lovelock, C.E., Ball, M.C., Feller, I.C., Engelbrecht, B.M.J., Ling Ewe, M., 2006. Variation in hydraulic conductivity of mangroves: Influence of species, salinity, and nitrogen and phosphorus availability. Physiologia Plantarum 127, 457–464. https://doi.org/10.1111/j.1399-3054.2006.00723.x

Lugo, A.F., Snedaker, S.C., 1974. The ecology of mangroves. Annual review of ecology and systematics 5, 39–64.

Méndez-alonzo, R., López-portillo, J., Moctezuma, C., Bartlett, M.K., Sack, L., 2016. Osmotic and hydraulic adjustment of mangrove saplings to extreme salinity. Tree Physiology 1–11. https://doi.org/10.1093/treephys/tpw073

Moschetto, F.A., Lopes, M.F., Silva, B.P., Lima Neto, M.C., 2019. Sodium benzoate inhibits germination, establishment and development of rice plants. Theoretical and Experimental Plant Physiology 31, 377–385. https://doi.org/10.1007/s40626-019-00151-z

Munns, R., Passioura, J.B., Colmer, T.D., Byrt, C.S., 2020. Osmotic adjustment and energy limitations to plant growth in saline soil. New Phytologist 225, 1091–1096. https://doi.org/10.1111/nph.15862

Murchie, E.H., Lawson, T., 2013. Chlorophyll fluorescence analysis: A guide to good practice and understanding some new applications. Journal of Experimental Botany 64, 3983–3998. https://doi.org/10.1093/jxb/ert208

Naidoo, G., 2006. Factors Contributing to Dwarfing in the Mangrove Avicennia marina 1095–1101. https://doi.org/10.1093/aob/mcl064

Nakano, Y., Asada, K., 1981. Hydrogen peroxide is scavenged by ascorbato specific peroxidase in spinach chloroplasts. Plant Cell Physiol 22, 867–880.

Neff, M.M., Chory, J., 1998. Genetic Interactions between Phytochrome A, Phytochrome B, and Cryptochrome 1 during Arabidopsis Development. PLANT PHYSIOLOGY 118, 27–35. https://doi.org/10.1104/pp.118.1.27

Reef, R., Lovelock, C.E., 2015. Regulation of water balance in mangroves 385–395. https://doi.org/10.1093/aob/mcu174

Schneider, C. a, Rasband, W.S., Eliceiri, K.W., 2012. NIH Image to ImageJ: 25 years of image analysis. Nature Methods 9, 671–675. https://doi.org/10.1038/nmeth.2089

Scholander, 1960. Sap Pressure in Vascular Plants. Science 148, 339–346.

Sobrado, M.A., 2000. Relation of water transport to leaf gas exchange properties in three mangrove species. Trees - Structure and Function 14, 258–262. https://doi.org/10.1007/s004680050011

Souza, G.M., Lüttge, U., 2015. Stability as a Phenomenon Emergent from Plasticity–Complexity–Diversity in Eco-physiology 211–239. https://doi.org/10.1007/978-3-319-08807-5_9

Souza, N.C.S., Silveira, J.A.G., Silva, E.N., Lima Neto, M.C., Lima, C.S., Ferreira-Silva, S.L., 2019. High CO 2 favors ionic homeostasis , photoprotection , and lower photorespiration in salt - stressed cashew plants. Acta Physiologiae Plantarum 1–14. https://doi.org/10.1007/s11738-019-2947-1

Vítolo, H.F., Souza, G.M., Silveira, J. a G., 2012. Cross-scale multivariate analysis of physiological responses to high temperature in two tropical crops with C \n 3 and C \n 4 metabolism. Environmental and Experimental Botany 80, 54–62. https://doi.org/10.1016/j.envexpbot.2012.02.002

Wang, C.-W., Wong, S.-L., Liao, T.-S., Weng, J.-H., Chen, M.-N., Huang, M.-Y., Chen, C.-I., 2022. Photosynthesis in response to salinity and submergence in two Rhizophoraceae mangroves adapted to different tidal elevations. Tree Physiology 42, 1016–1028. https://doi.org/10.1093/treephys/tpab167

Wang, W., Yan, Z., You, S., Zhang, Y., Chen, L., Lin, G., 2011. Mangroves: Obligate or facultative halophytes? A review. Trees - Structure and Function 25, 953–963. https://doi.org/10.1007/s00468-011-0570-x

Werner, A., Stelzer, R., 1990. Physiological responses of the mangrove Rhizophora mangle grown in the absence and presence of NaCl. Plant, Cell and Environment 13, 243–255. https://doi.org/10.1111/j.1365-3040.1990.tb01309.x

Yan, Z., Wang, W., Tang, D., 2007. Effect of different time of salt stress on growth and some physiological processes of Avicennia marina seedlings. Mar Biol 152, 581–587. https://doi.org/10.1007/s00227-007-0710-4

Zhou, M., Diwu, Z., Panchuk-Voloshina, N., Haugland, R.P., 1997. A Stable Nonfluorescent Derivative of Resorufin for the Fluorometric Determination of Trace Hydrogen Peroxide: Applications in Detecting the Activity of Phagocyte NADPH Oxidase and Other Oxidases. Analytical Biochemistry 253, 162–168. https://doi.org/10.1006/abio.1997.2391

Ziotti, A.B.S., Silva, B.P., Sershen, Lima Neto, M.C., 2019. Photorespiration is crucial for salinity acclimation in castor bean. Environmental and Experimental Botany 167, 103845. https://doi.org/10.1016/j.envexpbot.2019.103845

587

588

The plasticity of the photosynthetic apparatus and antioxidant responses are critical for the dispersion of *Rhizophora mangle* along a salinity gradient

Bruno Pereira Silva[a], Heloisa Maria Saballo[a], Ana Karla Moreira Lobo[b], Milton Costa Lima Neto[a*]

[a]São Paulo State University (UNESP). Biosciences Institute, Coastal Campus, São Vicente – SP, Brazil. PO box 73601 Zip Code: 11380-972

[b]Lancaster Environment Centre, Lancaster University, Lancaster, UK

*MCLN is the corresponding author. email: milton.lima-neto@unesp.br. Praça Infante Dom Henrique s/n. ZIP code 11.330-900, Parque Bitarú, São Vicente, SP, Brasil.

Abstract – The physiological mechanisms responsible for salinity tolerance in *Rhizophora mangle* remain unclear. Moreover, the effects of climate change on the distribution and abundance of mangrove forests are unknown. Thus, to elucidate the possible factors responsible for saline tolerance in this species, we investigated the growth and physiological parameters in young plants cultivated in a saline gradient (0, 10, 35, and 70 ppt). Biometric indicators, water status parameters, cell integrity, ions concentrations in leaves and roots, pigment concentrations, chlorophyll *a* fluorescence, oxidative stress indicators, and antioxidant enzyme activities were evaluated. The results showed that *R. mangle* could grow in the absence (0 ppt) or moderate salinity (10 ppt). However, by increasing the salinity to sea level (35 ppt), the growth and development decreased compared to plants grown at ten ppt. In hypersalinity (70 ppt), plant growth and development are severely hampered. Under hypersalinity, the increased concentration of H_2O_2 promoted lipid peroxidation and membrane damage. The chlorophyll contents decreased, and accessory pigment concentrations increased. Moreover, the modulation of the quantum yield of PSII and the antioxidant system was crucial to avoiding photoinhibition and salinity tolerance in *R. mangle.*

Keywords: antioxidant metabolism; climate change; mangroves; photosynthetic yield

Abbreviations: APX - ascorbate peroxidase; CAT – catalase; Fv/Fm – the potential yield of PSII; MD – membrane damage; NPQ – non-photochemical quenching; PPFD - photosynthetic photon flux density; PSII - photosystem II; PPFD - photosynthetic photon flux density, ppt – part per thousand; RWC – relative water content; TCC – total chlorophyll content; qL - estimation of the fraction of open PSII centers based on the lake model, rcf –

relative centrifuge force, SOD - superoxide dismutase, TBARS - thiobarbituric acid reactive substances; TCC – total chlorophyll; Y(II) – effective quantum yield of photosystem II; YNO – on-regulated non-photochemical energy loss; YNPQ – regulated non-photochemical energy loss

1 Introduction

Mangrove forests are distributed worldwide in tropical, subtropical, and semiarid coastline environments (Devaney et al., 2020) . Mangrove habitats are typically characterized by high salinity, tidal influence, strong winds, high temperature, and muddy anoxic soil (Wang et al., 2022). Several species co-exist in the mangrove environment and have different strategies to cope with such stressful conditions (Esteban et al., 2013). Moreover, mangrove forests are among the most carbon-rich ecosystems on Earth, storing vast amounts of soil carbon, which is crucial for the global carbon cycle and alleviating climate changes (Atwood et al., 2017) . Globally, mangrove communities are experiencing a change in soil salinity variation amplitude and flood depths due to sea-level rise and climate change. These conditions may impact mangrove seedlings' morphology and physiology, including growth, abundance, and distribution of this species composition (Wang et al., 2022).

Mangroves have intraspecific population variability in tolerance to abiotic stressors. The adaptations to flooding and salinity are the most critical factors that drive the local distribution of mangrove species (Méndez-alonzo et al., 2016) . Mangrove plants are well-adapted to salt concentrations that exceed the tolerated by most other plant species (Reef and Lovelock, 2015) . Several plant species co-exist in this environment and display different strategies to cope with salinity. The salt tolerance in mangroves ranges from functional obligate halophytes, which achieve their maximum growth at salinities from 5 to 25 ppt, to facultative halophytes and glycophytes, which optimize their growth in freshwater (Méndez-alonzo et al., 2016; Reef and Lovelock, 2015) . However, the literature has contradictory views regarding the obligated or facultative halophyte behaviour in mangroves (Adame et al., 2021; Cheeseman, 2015; Wang et al., 2011) .

Saline environments have a very negative water potential, making water absorption unfavourable. Consequently, the plant's ability to maintain water uptake in saline conditions is key to salt tolerance. Another physiological challenge to salinity exposure is ion toxicity (i.e. Na^+), as a high concentration is potentially cytotoxic to all plants, including mangroves (Reef and Lovelock, 2015) . Mangrove plants have evolved mechanisms to exclude, secrete and accumulate ions, such as the ultrafiltration of salt in the roots, the presence of salt glands, the hyper-accumulation of ions in the vacuoles, and the production of compatible solutes to osmotic adjustment (Esteban et al., 2013; Méndez-alonzo et al., 2016) .

In addition to salinity, mangroves are exposed to harmful stressors such as high light. Under these combined conditions, low stomatal conductance restricting photosynthesis can severely affect plant growth. The osmotic component of salinity decreases soil water potential, promoting stomatal closure and decreasing CO_2 supply for carboxylation in the chloroplasts (Cerqueira et al., 2019) . Secondly, the excessive ion accumulation decreases the efficiency of the Calvin-Benson-Bassham cycle reactions, leading to an imbalance between the production and consumption of the reducing equivalents produced by the photochemical reactions (Lima Neto et al., 2017) . Therefore, plants exposed to these conditions, commonly found in mangrove ecosystems, are prone to excess excitation energy accumulation in chloroplasts and photoinhibition.

The excess excitation energy in chloroplasts increases the production of reactive oxygen species (ROS) and induces oxidative stress. Thus, high salinity impairs photosynthesis by stomatal and metabolic limitations (Souza et al., 2019) . The increased concentration of ROS, produced by the excess excitation energy in chloroplasts, promotes photoinhibition on both photosystems (PSII and PSI) (Lima Neto et al., 2017) . Plants have evolved diverse photoprotective mechanisms to avoid the harmful effects of excess excitation energy and photoinhibition. Strategies to control the light interception by leaves are ubiquitous in plants, and these strategies can be achieved through different processes, such as changes in leaf orientation, leaf rolling, chloroplasts movements, and the presence of reflective structures such as wax, hairs, or salt crystals (Esteban et al., 2013) . In addition, plants have evolved different mechanisms to dissipate the excess excitation energy, such as non-photochemical quenching (NPQ), photorespiration (P_R), cyclic electron flow (CEF), and the water-water cycle (WWC). Moreover, the non-enzymatic and enzymatic antioxidants are crucial to maintaining cell redox homeostasis and scavenging excessive ROS (Cerqueira et al., 2019; Lima Neto et al., 2017; Ziotti et al., 2019) . However, little is known regarding the modulation of photoprotective mechanisms in mangrove species.

We hypothesized that the regulation of the photochemical yield and the antioxidant metabolism are essential to the growth of *Rhizophora mangle* in a saline gradient. We investigated the role of the modulation of PSII quantum yield and the antioxidant metabolism in *R. mangle* to salt tolerance. Biometric parameters, PSII quantum yields, and the antioxidative metabolism of *R. mangle* were evaluated in a salinity gradient. Knowledge of mangrove physiology and tolerance mechanisms to abiotic factors are crucial to conserving and reforestation efforts.

2 Material and Methods

2.1 Plant material and growth conditions

Mature, fresh propagules of *R. mangle* were collected from nearby trees in Cubatão Estuary (Cubatão, São Paulo, Brazil) and sorted by size and weight. Similar propagules were directly planted into pots (20 L) containing commercial substrate (Plantmax PXHA, Eucatex, SP, Brazil) and maintained in a growth chamber with controlled conditions [photosynthetic photon flux density (PPFD) of 400 µmol m^{-2} s^{-1}, temperature of 30ºC/26ºC day/night, relative humidity of ~65% and a 12 h photoperiod]. These controlled conditions mimicked a typical day in the Coastal region of Cubatão, São Paulo, Brazil (23º88'45" S, 46º42'09" W). Plants were cultivated under these conditions for 120 days and watered every two days with distilled water until pot saturation. Three times a week, the pots were supplemented with NaCl solution (10 ppt), and the electrical conductivity was measured to ensure the saline concentration in the substrate. This reference solution was set according to the salinity of the native environment where the propagules were harvested.

After the 120 days growth period, as described above, the plants were separated into four salinity groups: 0, 10, 35, and 70 ppt. These salinity levels are approximately equivalent of 0, 17.02, 53.07 and 96.91 mS/cm, at 25ºC, respectively or approximately 0, 171.11, 598.9 and 1197.8 mM NaCl, respectively. Plants were irrigated daily with their respective saline solutions. Weekly, the pots were abundantly rinsed with freshwater until drained to avoid salt over-accumulation in the substrate. The electrolyte leakage of the drained was measured weekly to maintain the substrate's salt concentration near the respective treatment concentration. Plants were grown under these conditions for 45 days (the time when plants exposed to 70 ppt presented loss of leaf turgor and chlorosis). Five plants were used for each treatment, and an experimental unit was represented by one plant in a 20 L^{-1} plastic pot.

2.2 Chlorophyll a fluorescence analysis

Chlorophyll *a* fluorescence was measured using the saturation pulse method with a portable chlorophyll fluorometer (JR-PAMIII WALZ, Effeltrich, Germany). Leaves were dark-adapted for 30 min for assessing Fo and Fm. Then, the leaves were exposed to actinic light (500 µmol m^{-2} s^{-1}) for at least 30 min to reach a photosynthetic steady state. The actinic light used was near the saturation point observed from previous light curves performed in our lab and close to the cabinet light intensity. The intensity and duration of the saturation

pulses were 8,000 µmol m^{-2} s^{-1} and 0.7 s, respectively. The following parameters were assessed: the potential quantum yield of PSII [Fv/Fm = (Fm-Fo)/Fm]; the effective quantum yield of PSII [YII = (Fm'- Fs)/Fm'], the proportion of opened (qL) and closed (1-qL) PSII states, the non-photochemical quenching [NPQ = (Fm – Fm')/Fm'], the quantum yield of non-regulated non-photochemical energy loss in PSII [Y(NO) = F/Fm] and the quantum yield of regulated non-photochemical energy loss in PSII [Y(NPQ) = F/Fm' - F/Fm]. Fm and Fo are the maximum and minimum fluorescence of dark-adapted leaves, respectively; Fm′ and Fs are the maximum and the steady state, respectively, fluorescence in the light-adapted samples (Klughammer and Schreiber, 2008; Murchie and Lawson, 2013).

2.3 Growth, biomass partition, relative water content, and water potential

Plants were evaluated for stem diameter at 2 cm from the soil with a pachymeter, the number of leaves, and plant height at the end of the experiment. The third expanded leaf, used for photosynthesis measurements, was photographed, and the leaf area was estimated using the software ImageJ (Schneider et al., 2012) . After the *in vivo* biometric measurements, the plants were harvested and separated into aboveground and roots, which were immediately weighed for fresh matter (FM).

The relative water content (RWC) was calculated from the fresh, turgid, and dry weights of leaves and roots (Lobo et al., 2015) . The dry matter (DM) was determined after 48 h in an oven at 75 °C, and the turgid weight was measured after six hours of saturation in deionized water at 7 °C in dark-condition. The leaf midday water potential (Ψw) was evaluated using a pressure chamber (3000 Scholander PWSC, ICT International, Armidale, AUS) (Scholander, 1960).

2.4 Membrane damage, lipid peroxidation, pigment contents, Na^+ and K^+ contents

The membrane damage, an indicator of cell integrity, was measured as described previously (Cerqueira et al., 2019) . Segments were placed in tubes containing 10 mL of deionized water and incubated in a shaking water bath for 24 h. After that, the electric conductivity of the medium was measured (L1). Then, the segments were boiled at 95^{o}C for 1h, cooled down to ambient temperature in an ice bath, and measured the electric conductivity (L2). The membrane damage (MD) was calculated as MD = (L1/L2) x 100 and expressed in %. The lipid peroxidation was assessed based on the formation of thiobarbituric acid-reactive substances (TBARS) (Cakmak and Horst, 1991) . The TBARS

concentration was calculated using the absorption coefficient (155 mM^{-1} cm^{-1}) and expressed as nmol MDA-TBA g^{-1} FM.

Chlorophyll a, b, total, and carotenoids were measured according to Lichtenthaler and Wellburn, 1983. Leaf samples were extracted in 80% cold acetone overnight at 7°C in dark-condition. After that, the samples were centrifuged at 10,000 rcf for 5 minutes. The supernatant was read in a spectrophotometer at different wavelengths as previously described (Lichtenthaler et al., 1983) . The total anthocyanin content was determined as previously described by (Neff and Chory, 1998) . Leaf segments were extracted in methanol and 1% HCl at 4°C overnight. After that, chloroform was added to the homogenate and centrifuged at 14,000 rcf for 5 min. The upper fraction was used for spectrophotometric reading at 530 and 657 nm. The total anthocyanins content was expressed as A530-A657 g^{-1} FW. Na^+ and K^+ contents were measured by flame photometry (Lima Neto et al., 2014) .

2.5 H_2O_2 content and enzymatic activities

The H_2O_2 content was measured by the Amplex Red Hydrogen Peroxide/Peroxidase Assay Kit (Invitrogen). Leaf segments were ground in K-phosphate buffer 100 mM (pH 7.5). The crude extract was centrifuged at 12,000 rcf for 30 min at 4 °C. According to the manufacturer protocol, the supernatant was supplemented with 10 mM Amplex-Red and 10 U of horseradish peroxidase. The resorufin production was measured at 560 nm in a spectrophotometer (Zhou et al., 1997) .

The enzymatic activities were assessed from a protein extract. Leaf segments were ground to a fine powder in liquid nitrogen and then extracted in 100 mM Tris-HCl buffer (pH 8.0) containing 30 mM DTT, 20% glycerol, 1 mM ascorbate, and 3% PEG-6000 (Lima Neto et al., 2017b) . The samples were centrifuged at 14,000 rcf for 20 minutes and stored at -20°C for enzymatic activity determination. The protein content was measured by the Bradford method (Bradford, 1976) using bovine serum albumin as standard.

Total ascorbate peroxidase (APX) activity (EC. 1.11.1.11) was measured following the ascorbate oxidation at 290 nm. The activity was assayed in a reaction mixture containing 0.5 mM ascorbate and 0.1 mM EDTA dissolved in 100 mM K-phosphate buffer (pH 7.0) and the enzyme extract. The reaction was started by adding 30 mM H_2O_2. The enzymatic activity was measured following the decrease in absorbance at 290 nm and 25 °C, over 300 s, and expressed as µmol ascorbate mg^{-1} protein min^{-1} (Nakano and Asada, 1981) . Total superoxide dismutase (SOD) activity (EC 1.15.1.1) was determined by measuring the

inhibition of the blue formazan production by the nitroblue tetrazolium chloride (NBT) photoreduction. SOD activity was measured by adding the leaf extract to a mixture containing 50 mM potassium phosphate buffer (pH 7.8), 0.1 mM EDTA, 13 mM L-methionine, 2 µM riboflavin, and 75 µM p-NBT in the dark. The reaction was carried out under illumination (30 W fluorescent lamp) at 25 °C for 6 min. The absorbance was measured at 540 nm (Giannopolotis and Ries, 1977) . One unit of SOD activity was defined as the amount of enzyme required to inhibit 50% of the NBT photoreduction, and activity was expressed as U mg protein min^{-1}. Total catalase (CAT) activity (EC 1.11.1.6) was measured following the oxidation of H_2O_2 at 240 nm. CAT activity was determined by the reaction of the crude enzyme extract in 50 mM potassium phosphate buffer (pH 7.0) containing 20 mM H_2O_2. The absorbance at 240 nm was measured over 300 s (Havir and McHale, 1987) , and CAT activity was calculated according to the molar extinction coefficient of H_2O_2 (36 mM cm^{-1}) and expressed as µmol H_2O_2 mg^{-1} protein min^{-1}.

2.6 Correlation-based network analysis

Correlation-based networks, including all physiological traits, were calculated using Pearson's product-moment correlation for each of the matrices of data from *R. mangle* under the four treatments (0, 10, 35, and 70 ppt). The nodes correspond to the physiological and biochemical evaluated parameters, and the links correspond to the strength of the connection between the nodes (in module) by Pearson correlation. Networks were designed by restricting the strength of the connections to a specific limit of Pearson correlation coefficient [(r) (-0,80 > r > 0,80)]. The parameters calculated from the networks were obtained as described by Assenov et al. (2008) . Correlation analyses were performed by Pearson correlation using the Correlation Calculator software (Basu et al., 2017) , and weighted correlation-based scale-free networks were calculated using MetScape 3 on Cytoscape v. 3.9.1.

2.7 Statistical analysis

The experiment was arranged in a completely randomized design, with four treatments (0, 10, 35, and 70 ppt NaCl) containing five replicates represented by one plant per pot. All dependent variables were analyzed by one-way *ANOVA* and the means were compared by Tukey's test ($P \leq 0.05$). Box plots show medians and first and third quartiles (25th and 75th percentiles), and whiskers extend from the hinge to the largest or smallest value, no further than 1.5 times. The statistical analyses shown in the plots were performed using R (version 4.0.2) and Rstudio version (1.3.959). Multivariate principal component analysis (*PCA*) was

performed on all analyzed dependents. Before *PCA* analysis, data were scaled to reduce the effect of different variables, allowing data standardization. The level of importance of each PC was determined by the broken-stick method (Vítolo et al., 2012) . The PCA was performed using the RFactoMineR and factoextra packages in R.

3 Results

3.1 Hypersalinity reduced growth, water status, $[K^+]/[Na^+]$ ratio and increased membrane damage in Rhizophora mangle

The total fresh plant biomass did not change in plants exposed to 0, 10, and 35 ppt. However, it was significantly decreased by 28% in plants exposed 70 ppt (hypersalinity) compared with plants grown under 10 ppt (the salinity of the environment where the plants were collected, called in this research as control) (Figure 1). Hypersalinity also negatively impacted the biomass partition compared to plants submitted to 10 ppt (control) (Figure 1). Plants grown in freshwater (~0 ppt) did not show significant differences in biomass allocation compared with plants grown under 10 ppt (Figure 1). Biometric parameters such as plant height, leaf area, and the number of leaves were also decreased by 35 ppt and hypersalinity (70 ppt), except the stem diameter, which was significantly increased compared to the control plants (plants grown in 10 ppt) (Table 1). However, these parameters did not change in plants grown in freshwater (~0 ppt) compared with the reference plants (10 ppt) (Table 1).

The relative water content (RWC) and membrane damage (MD) in leaves and roots were strongly affected by salinity (Figure 2). The RWC was decreased by 38% in leaves and 15% in roots, while MD significantly increased in both plant organs (~3-fold) in plants exposed to 70 ppt, compared to plants grown in 10 ppt (Figure 2). Freshwater (~0 ppt) significantly decreased the leaf RWC in leaves, but this parameter did not change in roots compared to the reference plants (10 ppt) (Figure 2 A-B). The membrane damage (MD) also increased in leaves and roots of plants grown in freshwater (~0 ppt) compared to control plants (10 ppt) (Figure 2 C-D).

The leaf water potential was significantly decreased by 65% in plants exposed to 70 ppt compared with control plants (10 ppt) (Figure 3A). In contrast, plants cultivated in freshwater (~0 ppt) did not change their water potential compared to control (Figure 3A). The leaf succulence presented the lowest value in plants grown in freshwater and the highest value in plants grown in 35 ppt. Moreover, the leaf succulence was not affected by hypersalinity (70 ppt) compared with control (Fig 3B). The $[K^+]/[Na^+]$ ratio significantly

increased in leaves and roots (2- and 6-fold, respectively) of plants grown in ~0 ppt. This ratio significantly decreased in leaves and roots of plants submitted to 35 and 70 ppt, all compared with control (Figure 3C-D). As expected, the $[K^+]/[Na^+]$ ratio significantly decreased as the salinity increased in a dose-response trend.

3.2 Photosynthetic pigment contents and PSII activity were severely affected by hypersalinity

The total chlorophyll content (*TCC*) was significantly reduced in plants exposed to 70 ppt, whereas it did not change in plants grown in freshwater compared to the reference plants (10 ppt). This parameter was lower in plants grown under 35 ppt than in the reference plants, and it did not change when compared to 70 ppt (Table 2). The chlorophyll a/b ratio significantly decreased in plants exposed to 35 ppt and *70 ppt* compared to the reference plants. In contrast, this ratio did not change in plants grown in freshwater compared to plants grown in 10 ppt (Table 2). The carotenoid content decreased by 39% in freshwater, and increased by 27% in 70 ppt compared with the control plants, respectively (Table 2). The anthocyanin content significantly increased by ~2-fold in plants exposed to 70 ppt, but did not change in freshwater plants compared with the reference plants (Table 2). These pigment changes contributed to modifications in PSII performance, especially in plants grown in hypersalinity, as described below.

The potential quantum yield of PSII (*Fv/Fm*) was not significantly affected in plants grown in different salinity conditions. This pattern shows that the plants were not photoinhibited (Figure 4A). The effective quantum yield of PSII [*Y(II)*] significantly reduced in plants exposed to 35 and 70 ppt. In contrast, *YII* was not affected by freshwater compared to the reference plants (Figure 4B). The open centers of PSII (*qL*) were only changed in plants exposed to 35 and 70, compared with the reference plants (10 ppt) (Figure 4C). In contrast, the non-photochemical quenching (NPQ) related parameters were enhanced by 35 and 70 ppt, respectively (Figure 5). The PSII closed centers (*1-qL*) and the NPQ increased in 35 and 70 ppt plants compared with reference plants (Figure 5A-B). The freshwater did not change these parameters compared to the reference plants (Figure 5A-B). The non-regulated non-photochemical energy loss of PSIII [*Y(NO)*] was higher in plants grown at 35 and 70 ppt than in the reference plants (10 ppt). This parameter did not change in plants submitted to freshwater compared with the reference plants (Figure 5C). Besides the *NPQ* did not change in plants grown in 35 ppt compared to 70 ppt, the non-regulated *NPQ (YNO)* was higher in plants under 70 ppt compared to plants grown in 35 ppt. In

contrast, the regulated portion of the *NPQ* [*Y(NPQ)*] significantly increased in plants grown in 35 ppt than in plants exposed to 70 ppt.

3.3 Oxidative stress indicators and antioxidant enzyme activities showed different patterns in response to freshwater and hypersalinity

To evaluate the aspects of the modulation of PSII quantum yields to photoprotection and the avoidance of ROS accumulation and oxidative stress, we evaluated lipid peroxidation, hydrogen peroxide content, and three major antioxidant enzyme activities. The lipid peroxidation, assessed by the thiobarbituric acid reactive substances (TBARS), increased as the salinity concentration became higher (Table 3). The H_2O_2 content in leaves followed the same trend as TBARS (Table 3). The superoxide dismutase (SOD) and catalase activities in leaves of *R. mangle* presented higher values as the NaCl concentration increased (Table 3). Plants grown in freshwater showed lower SOD, CAT, and ascorbate peroxidase (APX) activities than the reference plants (Table 3). The APX activity was lower in plants exposed to 70 ppt than in the reference plants and plants cultivated in 35 ppt (Table 3).

3.4 Systemic view of physiological indicators in R. mangle to different salinity

We performed a multivariate principal component analysis to summarize the information based on the many variables assessed and better understand the data set variation. The distribution of the variables determined in this study, including all treatments, is shown in Supplemental figure 1. PCA 1 and PCA 2 explained 80.6% of the total variance (Supplemental figure 1). The Na^+ content in leaves, anthocyanin concentration, YNO, H_2O_2 content, and Na^+ in roots were the main relevant variables for principal components 1 and 2. In contrast, Fv/Fm, total fresh matter, and leaf succulence were the less relevant variables for PC1 and PC2 (Supplemental figure 1). Additionally, the K^+ content in roots and leaves and the relative water content in roots showed a distinct behaviour compared with other variables, as essential components only in plants exposed to freshwater (0 ppt) (Supplemental figure 1). There was a clear distribution pattern among treatments, with each treatment separated into a distinct quadrant (Supplemental figure 1).

The weighted correlation-based network analysis (WCNA) presented well-defined differences in plants exposed to freshwater and 10 ppt, compared with plants grown under 35 and 70 ppt (Supplemental figure 2). Plants grown under freshwater or 10 ppt presented more loosened networks than plants under 35 and 70 ppt. Moreover, plants under 70 ppt

showed the highest network centralization (Supplemental table 1). Control plants grown in 10 ppt showed the highest number of nodes, edges, average number of neighbours, clustering coefficient, and network density (Supplemental table 1). In contrast, the network parameters from plants grown under 35 ppt showed the lowest values of the number of edges, average number of neighbours, clustering coefficient, network density, heterogeneity, and centralization (Supplemental table 1).

4 Discussion

4.1 Rhizophora mangle showed similar growth in freshwater and low salinity, but it was severely affected by hypersalinity, a common pattern of facultative halophytes

Although *R. mangle* is commonly considered a halophyte species, there are contradictory views regarding the relationship between mangroves and salt stress in the literature (Wang et al., 2011) . Some authors argue that mangroves are considered facultative halophytes, as freshwater is a physiological requirement while saltwater is an ecological requirement (Krauss and Ball, 2013) . This latter condition prevents the invasion and competition with non-halophyte plants for the restricted resources in the mangrove environment. In contrast, some reports describe mangroves as obligate halophytes, which cannot grow in permanent freshwater; consequently, salt is a physiological requirement (Lugo and Snedaker, 1974) . Nevertheless, *R. mangle* plants are sensitive to hypersalinity. It is important to note that there is no consensus in the literature regarding mangrove's hypersalinity threshold. However, according to Devaney et al. (2020) , hypersaline conditions range from salt concentrations above 50 ppt, which corroborates with the salinities used in this research as hypersalinity (70 ppt).

In our study, *R. mangle* exposed to hypersalinity showed lower plant height, less biomass accumulation and leaf area, and a lower number of leaves compared with plants grown in a saline concentration equivalent to their natural environment (10 ppt) or compared to plants grown in freshwater (Table 1 and Figure 1). In opposition, the stem diameter was significantly increased in plants exposed to hypersalinity (Table 1). These parameters were not affected in plants cultivated in freshwater (0 ppt) compared with plants exposed to 10 ppt. Growth performance is a sensitive indicator of tolerance in plants exposed to salinity. Non-halophytes survive optimally in freshwater and mortality is imminent at slightly higher salinity concentrations. Facultative halophytes can also grow in freshwater but differ from non-halophytes in responding to increases in salinity with promoted growth, up to an optimum level, above which growth would decrease. Finally, obligate halophytes have

optimal growth under ranges of salinity similar or greater to those of facultative halophytes but differ in their inability to survive under freshwater (Cheeseman, 2015; Flowers and Colmer, 2015, 2008; Krauss and Ball, 2013; Wang and Yan, 2011) . Therefore, it suggests that *R. mangle* is a facultative halophyte, as it can survive in freshwater, even though its growth was slightly reduced.

4.2 Osmotic protection and ion partitioning maintain an optimum water status and cellular integrity under hypersalinity in R. mangle

R. mangle plants can grow and flower regularly when irrigated with freshwater (Wang and Yan, 2011; Werner and Stelzer, 1990) . Plants grown in 35 ppt or 70 ppt showed significant alterations in biometric parameters (Figure 1 and Table 1). These biometric alterations induced by 35 ppt and 70 ppt are related to the reduced leaf water potential and the relative imbalance in the $[K^+]/[Na^+]$ ratio in leaves and roots (Figure 3). It was previously shown that *R. mangle* could keep extremely low leaf water potentials (-5 MPa), maintaining their hydraulic system safe (Méndez-alonzo et al., 2016) . Hence, the higher stem diameter in plants exposed to 35 and 70 ppt could be related to a better hydraulic conductivity efficiency in low water potential (Méndez-alonzo et al., 2016).

Maintaining an efficient stem hydraulic system is important to ensure the hydraulic conductivity of leaves under low water potential, sustaining transpiration and photosynthesis. Mangroves typically have relatively low transpiration rates and high water use efficiencies (Lovelock et al., 2006) . Lower stomatal conductance resulting from increasing substrate salinity in mangroves is well established; when soil salinity is greater than the seawater salt concentration (35 ppt), the whole-plant hydraulic conductance can decline due to xylem cavitation, resulting in severe limitations of photosynthesis and growth (Méndez-alonzo et al., 2016) , which is in accordance with our data. *R. mangle* leaves also showed higher water content per unit area (leaf succulence) under salinity conditions than in plants cultivated in freshwater (0 ppt) (Fig. 3). This response corroborates with previous research, suggesting that leaf succulence increases as salinity rises (Camilleri and Ribi, 1983) .

Mangroves have relatively low photosynthetic carbon gain and reduced productivity. Decreased number of leaves, leaf area, and height could be energetically efficient in this species under salt stress (Munns et al., 2020) . As an osmotic effect of the salt stress, the stomatal closing decreases leaf transpiration, water intake, and, consequently, salt intake. This physiological response of tolerant species avoids the toxic effects of the excess Na^+

concentration in the leaf tissue (Flowers and Colmer, 2008). However, the CO_2 assimilation is decreased by stomatal limitation, consequently promoting the excess excitation energy in the chloroplasts, as the Calvin-Benson-Bassham cycle reactions are the main sink of the reducing equivalents produced by the photochemical reactions (Cerqueira et al., 2019). Thus, increases in the water content in leaves exposed to salinity (salt succulence) enhance the leaf's capacity to dissipate heat, reducing the need for evaporative cooling. This is an important mechanism in plants under stomatal closing as *R. mangle* under hypersalinity (Calzadilla et al., 2022).

Like many other halophytes, mangroves use the accumulation of select ions as solutes to adjust the osmotic potential (Reef and Lovelock, 2015), which is in accordance with our data (Figure 3). However, in mangroves growing at high salinity, the predicted shoot osmotic potential, calculated from cellular ion concentrations, is higher than the observed one (Méndez-alonzo et al., 2016). Therefore, above the hypersalinity threshold, other compatible osmotic substances are necessary to reduce the water potential and maintain water uptake. The membrane damage, an indicator of cell integrity, was increased in plants exposed to hypersalinity and slightly increased in plants cultivated in freshwater compared with reference plants (Figure 2), corroborating the importance of osmotic adjustment to cell integrity.

Low salinity maintained cell integrity in *R. mangle* compared with plants cultivated in 0, 35, and 70 ppt (Figure 2). Probably, low salinity was able to induce osmotic protection by the accumulation of compatible solutes, which could promote cell organelles protection and whole-cell integrity. However, little is known regarding the metabolism of the accumulation of organic compatible solutes to salt acclimated-*R. mangle* and its influence on salt acclimation (Munns et al., 2020). *R. mangle* plants cultivated in freshwater showed a significant Na^+ concentration in leaves and roots (Figure 3). This could be explained as viviparous mangroves, as *R. mangle* have larger propagules that store large amounts of nutrients and energy (Yan et al., 2007) and high concentrations of Na^+ and Cl^- (Wang and Yan, 2011). Thus, even growing in freshwater in the short term, *Rhizophora* seedlings still have significant concentrations of Na^+ and Cl^-.

4.3 The plasticity and resilience of the photosynthetic apparatus of R. mangle under salinity

The modulation of the photosynthetic PSII quantum yields was evaluated by chlorophyll *a* fluorescence analysis. The potential quantum yield of photosystem II (PSII) (Fv/Fm), an indicator of the maximum photosynthetic yield, did not change in plants exposed

to hypersalinity or the absence of NaCl compared to the reference plants (Figure 4). Roughly, high Fv/Fm could indicate that PSII is not photoinhibited. However, to avoid photoinhibition, this species should modulate the use and efficiency of the different quantum yields of both photosystems (Lima Neto et al., 2017b).

Under photoinhibited conditions, $P680^{+}$ lifetime increases, and this powerful oxidant may degrade pigments and amino acids nearby. On the other hand, when the acceptor side is less efficient, a P680 triplet radical is formed, interacting with atmospheric oxygen (O_2), forming singlet oxygen ($^1O_2$). These reactive oxygen species degrade D1 protein in the core of the PSII reaction center (Lima Neto et al., 2017b). As a response to hypersalinity, *R. mangle* plants significantly decreased the effective quantum yield of PSII [Y(II)] compared with plants exposed to the reference treatment and freshwater (Fig. 4). Also, plants under hypersalinity displayed a higher portion of reduced Qa, indicated by the decrease in qL, showing a closed state of PSII by an acceptor site limitation (Cerqueira et al., 2019). Hence, the decrease in Y(II) by plants exposed to hypersalinity was followed by the increase in the closed state of Qa (1-qL) (Figure 5), indicating an acceptor site limitation of PSII. Denvaney et al. (2020) showed that Y(II) changes in *R. mangle* were not significantly related to soil salinity. However, where soils were hypersaline (ranging from 55 to 78 ppt), the Y(II) strongly decreased as soil salinity enhanced. Also, at soil salinities >60 ppt, Y(II), growth and the survival of *R. mangle* seedlings were severely reduced (Devaney et al., 2020), which is in accordance with our data. Previous works have demonstrated that photoinhibition occurs in hypersaline conditions for several species (Biber, 2006; Naidoo, 2006; Sobrado, 2000).

R. mangle exposed to hypersalinity strongly induced the dissipation of excess excitation energy by the non-photochemical quenching (NPQ) (Figure 5). This mechanism protects the reaction centers of PSII via rapid dissipation of excess excitation energy as heat. It is essential to mention that the PSII quantum yield efficiency can be decreased by damaging the PSII reaction center or inducing NPQ (Areington et al., 2022). The contribution of these aspects to the NPQ increase was estimated by the evaluation of the quantum yield of the non-regulated [Y(NO)] and regulated [Y(NPQ)] non-photochemical energy losses in PSII. It was shown that the regulated NPQ portion was the relatively most crucial component of the increase in NPQ in *R. mangle* exposed to hypersalinity (Figures 5C-D).

Corroborating these previous results, the carotenoid and anthocyanin contents, both pigments involved in photoprotection, were increased in *R. mangle* exposed to 70 ppt (Table 2). Moreover, the chlorophyll contents were decreased in plants exposed to 70 ppt, probably

to reduce light-harvesting and consequently excess excitation energy in the chloroplasts. Even with the decrease in chlorophyll content, plants exposed to hypersalinity tended to present a lower chlorophyll a/b ratio, which may be involved with a photoprotection mechanism to avoid light-harvesting and, consequently, excess excitation energy in chloroplasts (Lima Neto et al., 2017b).

4.4 The dissipation of excess excitation energy in chloroplasts was not able to avoid oxidative stress in R. mangle exposed to hypersalinity

The lipid peroxidation and H_2O_2 were increased due to the increased NaCl concentration (Table 3). The over-reduction of the electron transport chain in mitochondria and chloroplasts are the main sites of ROS production. Plants have evolved different metabolic strategies to scavenge excess ROS. In particular, ROS is involved with signalling processes, but the excess constantly challenges the chloroplast during photochemical reactions. The disruption of the balance between the photochemical reactions, producing the reducing equivalents and their consumption by the Calvin-Benson-Bassham cycle, is a prominent situation of ROS production, promoting photoinhibition (Lima Neto et al., 2017b). Thus, the balance between ROS production and their removal by enzymatic and non-enzymatic antioxidants determines the type and concentration of ROS present and to what extent damage will occur (Foyer et al., 2017).

R. mangle plants exposed to elevated salt concentrations increased the SOD and CAT activities in leaves (Table 3). These enzymes work in a synchronized way, forming an efficient antioxidant system. The SOD will catalyze the scavenging of the superoxide radical, forming H_2O_2 which is further removed by CAT. Thus, in our data, the activities of these enzymes are positively correlated and work together to remove the excess ROS produced by the effects of high salinity. On the other hand, the APX activity was higher in the reference plants, and its activity was decreased in plants exposed to freshwater and hypersalinity (Table 3). It was previously shown that salt enhanced SOD activity, which was not matched by APX activity (Gueta-Dahan et al., 1997). Moreover, these authors suggest that APX is a salt-sensitive enzyme, inhibited by the excess of H_2O_2 (Moschetto et al., 2019). Thus, in our study, the increase in the H_2O_2 content produced by hypersalinity probably impaired the activity of APX in *R. mangle*.

4.5 Physiological network plasticity promotes tolerance to different ranges of salinity in Rhizophora mangle

The responses of plants to environmental complexity are the sum of their modular responses and all the interaction effects resulting from the integration of individual modules, which allows emergent properties of biological systems (Souza and Lüttge, 2015). Thus, no single scale can represent whole-plant plasticity (Bertolli et al., 2013; Vítolo et al., 2012). The functional plasticity in *R. mangle* plants is given by multifunctional regulatory capacity, permitting performance variations in different saline conditions. It is based on network structures and topology providing high degrees of flexibility (Supplemental Table 1 and Supplemental Figure 1).

Our data clearly show that plants exposed to different saline levels could adjust different morphometric and physiological responses to acclimation (Supplemental Figures 1 and 2). Plants exposed to freshwater or low salinity (10 ppt) presented more approximated network topologies when compared with plants exposed to 35 and 70 ppt (Supplemental Figure 2 and Supplemental Table 1). These data show a systemic view of the acclimation responses of *R. mangle* as an integrated response with the interaction and flux of energy and information among different modules and physiological responses.

5. Conclusions

This study demonstrates that saline acclimation and tolerance of *Rhizophora mangle* is a complex phenomenon influenced by an integrated variety of metabolic and physiological responses. *R. mangle* plants can grow and develop in the presence of freshwater (absence of salt) and moderate salinity. In contrast, under hypersaline conditions, growth and biomass accumulation is impaired. In response to hypersalinity, the biomass partition and the accumulation of ions and compatible solutes are modulated to maintain the water status. Moreover, the plasticity in the efficiency of the quantum yields on PSII is crucial to dissipate the excess excitation energy avoiding photoinhibition in *R. mangle* exposed to hypersalinity.

Plants grown under constant salinity in a laboratory setting are unlikely to behave similarly to those in their natural habitat with fluctuating salinity. Thus, studies on the effects of freshwater, low salinity, and salinity fluctuation on mangroves and the physiological mechanisms under fluctuating salinity conditions should be strengthened in future research.

Authors contribution section

BPS, **HMS,** and **YB**: investigation, validation, formal analysis. **AKML**: formal analysis, review & editing, visualization. **MCLN**: conceptualization, methodology, resources, writing original draft, review & editing, supervision, funding acquisition, and project administration.

Declaration of competing interest

The authors declare that they have no competing financial interests or personal relationships that could have appeared to influence the work reported in this paper.

Acknowledgments/Funding

The authors would like to thank the financial support from grants #2019/26850-7 AKML, #201919245-0 HMS and #2018/04258-6 MCLN, São Paulo Research Foundation (FAPESP) and grant #404707/2018-1, National Council for Scientific and Technological Development CNPq, MCLN.

Figure Captions

Figure 1- Biomass partition (aboveground and root) of *Rhizophora mangle* exposed to 0, 10, 35 and 70 ppt NaCl in a growth chamber. Data represent the means (bars and numbers in white) and standard deviation of five biological replicates. According to Tukey's test, different letters represent significant differences between treatments ($P \leq 0.05$).

Figure 2 - Leaf (A, C) and root (B, D) relative water content and membrane damage of *Rhizophora mangle* exposed to 0, 10, 35 and 70 ppt NaCl. Boxes represent the median and first and third quartiles (n = five biological replicates), and whiskers represent the standard deviation. According to Tukey's test, different letters represent significant differences between treatments ($P \leq 0.05$).

Figure 3: Leaf water potential (A) and succulence (B), and the $[K^+]/[Na^+]$ ratio in leaves (C) and roots (D) of *Rhizophora mangle* exposed 0, 10, 35 and 70 ppt NaCl. Boxes represent the median and first and third quartiles (n = five biological replicates) and whiskers represent the standard deviation. According to Tukey's test, different letters represent significant differences between treatments ($P \leq 0.05$).

Figure 4: Potential quantum yield of PSII (A), effective quantum yield of PSII (B), and open PSII centers (D) of leaves of *Rhizophora mangle* exposed to 0, 10, 35 and 70 ppt NaCl. Boxes represent the median and first and third quartiles (n= five biological replicates) and whiskers represent the standard deviation. According to Tukey's test, different letters represent significant differences between treatments ($P \leq 0.05$).

Figure 5: Closed PSII centers (A), non-photochemical quenching (B), quantum yield of non-regulated (C), and regulated (D) non-photochemical energy loss of PSII of leaves of *Rhizophora mangle* exposed to 0, 10, 35 and 70 ppt NaCl. Boxes represent the median and first and third quartiles (n = five biological replicates) and whiskers represent the standard deviation. According to Tukey's test, different letters represent significant differences between treatments ($P \leq 0.05$).

Figure S1: PCA ordination diagram of variables plots with significant variation across salinity levels. The two axes (PCA 1 and 2) explained 80.6% of the variance. The percentage of variation explained by each principal component is shown. Red circles represent plants grown at 70 ppt NaCl. Orange circles represent plants grown at 35 ppt NaCl. Yellow circles represent plants grown at 10 ppt NaCl and green circles, plants grown in freshwater. Variable caption: rwc_leaf is the relative water content in leaves, rwc_root is the relative water content in roots, tfm is the total fresh matter, wpot is the water potential, k_leaf and k_root are the K^+ content in leaves and roots respectively, md_leaf and md_roots are the membrane damage in leaves and roots respectively, car is the carotenoid content in leaves, diameter is the stem diameter, na_leaf and na_root are the Na+ contents in leaves and roots respectively.

Figure S2: Correlation-based networks of physiological parameters in *R. mangle* plants cultivated in freshwater (A), 10 ppt NaCl (B), 35 ppt NaCl (C) and 70 ppt NaCl (D). Nodes represent physiological parameters and lines their pairwise correlations. Blue links represent a positive correlation and red links represent a negative correlation. Ticker links indicate a higher correlation in module (n = 5).

570 **Table 1**: Plant height, stem diameter, leaf area and number of leaves of Rhizophora mangle exposed
571 to salinity levels in a growth chamber. Values represent the mean ± SD of five biological replicates
572 (n = 5). According to Tukey's test, different letters represent significant differences between
573 treatments (P ≤ 0.05)

574

	0	10	35	70
Plant height (cm plant^{-1})	48.84 ± 1.73a	51.85 ± 1.96a	40.42 ±1.08b	36.06 ± 1.52b
Stem diameter (cm plant^{-1})	8.20 ± 0.66b	10.30 ± 0.67b	13.27 ± 0.44a	13.04 ± 0.48a
Leaf area (cm^2)	43.29 ± 2.58a	42.68 ± 2.87ab	33.68 ± 1.27bc	24.78 ± 1.03c
Number of leaves (plant^{-1})	14.00 ± 0.58a	12.33 ± 0.33ab	10.67 ± 0.67b	7.67 ± 0.33c

575

576 **Table 2:** Total chlorophyll content, chlorophyll a/b ratio, carotenoids and anthocyanin contents in
577 leaves of *Rhizophora mangle* exposed to increasing salinity. Values represent the mean ± SD of five
578 biological replicates (n = 5). According to Tukey's test, different letters represent significant
579 differences among treatments (P ≤ 0.05).

	0	10	35	70
Total Chl (mg g^{-1} FM)	99.21 ± 7.75a	94.95 ± 6.97a	67.85 ± 1.50b	56.52 ± 2.62b
Chl a/Chl b ratio	2.40 ± 0.30a	2.00 ± 0.03a	1.38 ± 0.08b	1.53 ± 0.06b
Carotenoids (mg g^{-1} FM)	95.54 ± 3.19c	152.16 ± 9.20b	174.60 ± 4.45b	193.54 ± 4.70a
Anthocyanin (mg g^{-1} FM)	0.98 ± 0.07b	1.19 ± 0.04b	2.01 ± 0.07a	2.28 ± 0.14a

580

Table 3: Contents of TBARS (lipid peroxidation) and H_2O_2, and the activities of superoxide dismutase, ascorbate peroxidase and catalase in leaves of *Rhizophora mangle* exposed to increasing salinity. Values represent the mean ± SD of five biological replicates (n = 5). According to Tukey's test, different letters represent significant differences among treatments ($P \leq 0.05$).

	0	**10**	**35**	**70**
TBARS content (nmol MDA-TBA g^{-1} FM)	42.91 ± 4.70c	85.39 ± 4.08b	97.40 ± 2.65ab	106.09 ± 3.99a
H_2O_2 content (ηmol g^{-1} FM)	12.04 ± 0.38c	30.74 ± 1.14b	44.53 ± 2.00a	47.12 ± 0.52a
SOD activity (U mg^{-1} protein min^{-1})	2.58 ± 0.40c	3.87 ± 0.38bc	5.55 ± 0.32ab	6.34 ± 0.45a
APX activity (mmol mg^{-1} protein min^{-1})	0.81 ± 0.09c	2.76 ± 0.20b	3.87 ± 0.37a	1.04 ± 0.02c
CAT activity (mmol mg^{-1} protein min^{-1})	95.54 ± 3.19c	152.16 ± 9.20b	174.60 ± 4.45ab	193.54 ± 4.70a

586 **References**

Adame, M.F., Reef, R., Santini, N.S., Najera, E., Turschwell, M.P., Hayes, M.A., Masque, P., Lovelock, C.E., 2021. Mangroves in arid regions: Ecology, threats, and opportunities. Estuarine, Coastal and Shelf Science 248, 106796. https://doi.org/10.1016/j.ecss.2020.106796

Areington, C.A., Lima Neto, M.C., Watt, P.M., Sershen, 2022. Assessing the utility of selected photosynthetic and related traits in screening Amaranthus dubius Mart. ex Thell. and Galinsoga parviflora Cav. 1796 seedlings for elevated temperature stress tolerance. South African Journal of Botany 000. https://doi.org/10.1016/j.sajb.2022.02.037

Assenov, Y., Ramírez, F., Schelhorn, S.E.S.E., Lengauer, T., Albrecht, M., 2008. Computing topological parameters of biological networks. Bioinformatics 24, 282–284. https://doi.org/10.1093/bioinformatics/btm554

Atwood, T.B., Connolly, R.M., Almahasheer, H., Carnell, P.E., Duarte, C.M., Ewers Lewis, C.J., Irigoien, X., Kelleway, J.J., Lavery, P.S., Macreadie, P.I., Serrano, O., Sanders, C.J., Santos, I., Steven, A.D.L., Lovelock, C.E., 2017. Global patterns in mangrove soil carbon stocks and losses. Nature Climate Change 7, 523–528. https://doi.org/10.1038/nclimate3326

Basu, S., Duren, W., Evans, C.R., Burant, C.F., Michailidis, G., Karnovsky, A., 2017. Sparse network modeling and metscape-based visualization methods for the analysis of large-scale metabolomics data. Bioinformatics 33, 1545–1553. https://doi.org/10.1093/bioinformatics/btx012

Bertolli, S.C., Vítolo, H.F., Souza, G.M., 2013. Network connectance analysis as a tool to understand homeostasis of plants under environmental changes. Plants 2, 473–488. https://doi.org/10.3390/plants2030473

Biber, P.D., Biber, P.D., 2006. Measuring the effects of salinity stress in the red mangrove, Rhizophora mangle L. African Journal of Agricultural Research 1, 001–004.

Bradford, M.M., 1976. A rapid and sensitive method for the quantification of microgram quantities of protein utilizing the principle of protein-dye binding. Analytical Biochemistry 722, 248–254.

Cakmak, I., Horst, W.J., 1991. Effect of aluminium on lipid peroxidation, superoxide dismutase, catalase, and peroxidase activities in root tips of soybean (Glycine max). Physiologia Plantarum 83, 463–468. https://doi.org/10.1111/j.1399-3054.1991.tb00121.x

Calzadilla, P.I., Carvalho, F.E.L., Gomez, R., Lima Neto, M.C., Signorelli, S., 2022. Assessing photosynthesis in plant systems: A cornerstone to aid in the selection of resistant and productive crops. Environmental and Experimental Botany 201, 104950. https://doi.org/10.1016/j.envexpbot.2022.104950

Camilleri, J.C., Ribi, G., 1983. Leaf Thickness of Mangroves (Rhizophora mangle) Growing in Different Salinities. Biotropica 15, 139. https://doi.org/10.2307/2387959

Cerqueira, J.V.A., Silveira, J.A.G., Carvalho, F.E.L., Cunha, J.R., Lima Neto, M.C., 2019. The regulation of P700 is an important photoprotective mechanism to NaCl-salinity in Jatropha curcas. Physiologia Plantarum. https://doi.org/10.1111/ppl.12908

Cheeseman, J.M., 2015. The evolution of halophytes, glycophytes and crops, and its implications for food security under saline conditions. New Phytologist 206, 557–570. https://doi.org/10.1111/nph.13217

Devaney, J.L., Marone, D., Mcelwain, J.C., 2020. Impact of soil salinity on mangrove restoration in a semiarid region : a case study from the Saloum Delta , Senegal 29, 1–10. https://doi.org/10.1111/rec.13186

Esteban, R., Fernández-Marín, B., Hernandez, a., Jiménez, E.T., León, a., García-Mauriño, S., Silva, C.D., Dolmus, J.R., Dolmus, C.M., Molina, M.J., Gutierrez, N.N., Loaisiga, M.I., Brito, P., García-Plazaola, J.I., 2013. Salt crystal deposition as a reversible mechanism to enhance photoprotection in black mangrove. Trees - Structure and Function 27, 229–237. https://doi.org/10.1007/s00468-012-0790-8

Flowers, T.J., Colmer, T.D., 2015. Plant salt tolerance: adaptations in halophytes. Annals of Botany 115, 327–331. https://doi.org/10.1093/aob/mcu267

Flowers, T.J., Colmer, T.D., 2008. Salinity tolerance in halophytes. The New phytologist 179, 945–63. https://doi.org/10.1111/j.1469-8137.2008.02531.x

Foyer, C.H., Ruban, A.V., Noctor, G., 2017. Viewing oxidative stress through the lens of oxidative signalling rather than damage. Biochemical Journal 474, 877–883. https://doi.org/10.1042/BCJ20160814

Giannopolotis, C.N., Ries, S.K., 1977. Superoxide dismutases: Occurrence in higher plants. Plant Physiology 59, 309–314.

Gomes Soares, M.L., Pereira Tognella, M.M., Cuevas, E., Medina, E., 2015. Photosynthetic capacity and intrinsic water-use efficiency of Rhizophora mangle at its southernmost western Atlantic range. Photosynthetica 53, 464–470. https://doi.org/10.1007/s11099-015-0119-0

Gueta-Dahan, Y., Yaniv, Z., Zilinskas, B.A., Ben-Hayyim, G., 1997. Salt and oxidative stress: similar and specific responses and their relation to salt tolerance in Citrus. Planta 203, 460–469. https://doi.org/10.1007/s004250050215

Havir, E.A., McHale, N.A., 1987. Biochemical and Developmental Characterization of Multiple Forms of Catalase in Tobacco Leaves. Plant Physiology 84, 450–455. https://doi.org/10.1104/pp.84.2.450

Klughammer, C., Schreiber, U., 2008. Complementary PS II quantum yields calculated from simple fluorescence parameters measured by PAM fluorometry and the Saturation Pulse method. PAM Application Notes 1, 27–35. https://doi.org/citeulike-article-id:6352156

Krauss, K.W., Ball, M.C., 2013. On the halophytic nature of mangroves. Trees 27, 7–11. https://doi.org/10.1007/s00468-012-0767-7

Lichtenthaler, H., Wellburn, A., Lichtentharler, H.K., Welburn, A.R., 1983. Determination of total carotenoids and chlorophylls a and b of leaf extracts in different solvents. Biochemical Society Transactions 11, 591–592. https://doi.org/10.1042/bst0110591

Lima Neto, M.C., Cerqueira, J.V.A., Cunha, J.R., Ribeiro, R.V., Silveira, J.A.G., 2017a. Cyclic electron flow, NPQ and photorespiration are crucial for the establishment of young plants of Ricinus communis and Jatropha curcas exposed to drought. Plant Biology 19, 650–659. https://doi.org/10.1111/plb.12573

Lima Neto, M.C., Lobo, A.K.M., Martins, M.O., Fontenele, A.V., Silveira, J.A.G., 2014. Dissipation of excess photosynthetic energy contributes to salinity tolerance: A comparative study of salt-tolerant Ricinus communis and salt-sensitive Jatropha curcas. Journal of Plant Physiology 171, 23–30. https://doi.org/10.1016/j.jplph.2013.09.002

Lima Neto, M.C., Silveira, J.A.G., Cerqueira, J.V.A., Cunha, J.R., 2017b. Regulation of the photosynthetic electron transport and specific photoprotective mechanisms in Ricinus communis under drought and recovery. Acta Physiologiae Plantarum 39, 183. https://doi.org/10.1007/s11738-017-2483-9

Lobo, A.K.M., de Oliveira Martins, M., Lima Neto, M.C., Machado, E.C., Ribeiro, R.V., Silveira, J.A.G., 2015. Exogenous sucrose supply changes sugar metabolism

and reduces photosynthesis of sugarcane through the down-regulation of Rubisco abundance and activity. Journal of Plant Physiology 179, 113–121. https://doi.org/10.1016/j.jplph.2015.03.007

Lovelock, C.E., Ball, M.C., Feller, I.C., Engelbrecht, B.M.J., Ling Ewe, M., 2006. Variation in hydraulic conductivity of mangroves: Influence of species, salinity, and nitrogen and phosphorus availability. Physiologia Plantarum 127, 457–464. https://doi.org/10.1111/j.1399-3054.2006.00723.x

Lugo, A.F., Snedaker, S.C., 1974. The ecology of mangroves. Annual review of ecology and systematics 5, 39–64.

Méndez-alonzo, R., López-portillo, J., Moctezuma, C., Bartlett, M.K., Sack, L., 2016. Osmotic and hydraulic adjustment of mangrove saplings to extreme salinity. Tree Physiology 1–11. https://doi.org/10.1093/treephys/tpw073

Moschetto, F.A., Lopes, M.F., Silva, B.P., Lima Neto, M.C., 2019. Sodium benzoate inhibits germination, establishment and development of rice plants. Theoretical and Experimental Plant Physiology 31, 377–385. https://doi.org/10.1007/s40626-019-00151-z

Munns, R., Passioura, J.B., Colmer, T.D., Byrt, C.S., 2020. Osmotic adjustment and energy limitations to plant growth in saline soil. New Phytologist 225, 1091–1096. https://doi.org/10.1111/nph.15862

Murchie, E.H., Lawson, T., 2013. Chlorophyll fluorescence analysis: A guide to good practice and understanding some new applications. Journal of Experimental Botany 64, 3983–3998. https://doi.org/10.1093/jxb/ert208

Naidoo, G., 2006. Factors Contributing to Dwarfing in the Mangrove Avicennia marina 1095–1101. https://doi.org/10.1093/aob/mcl064

Nakano, Y., Asada, K., 1981. Hydrogen peroxide is scavenged by ascorbato specific peroxidase in spinach chloroplasts. Plant Cell Physiol 22, 867–880.

Neff, M.M., Chory, J., 1998. Genetic Interactions between Phytochrome A, Phytochrome B, and Cryptochrome 1 during Arabidopsis Development. PLANT PHYSIOLOGY 118, 27–35. https://doi.org/10.1104/pp.118.1.27

Reef, R., Lovelock, C.E., 2015. Regulation of water balance in mangroves 385–395. https://doi.org/10.1093/aob/mcu174

Schneider, C. a, Rasband, W.S., Eliceiri, K.W., 2012. NIH Image to ImageJ: 25 years of image analysis. Nature Methods 9, 671–675. https://doi.org/10.1038/nmeth.2089

Scholander, 1960. Sap Pressure in Vascular Plants. Science 148, 339–346.

Sobrado, M.A., 2000. Relation of water transport to leaf gas exchange properties in three mangrove species. Trees - Structure and Function 14, 258–262. https://doi.org/10.1007/s004680050011

Souza, G.M., Lüttge, U., 2015. Stability as a Phenomenon Emergent from Plasticity–Complexity–Diversity in Eco-physiology 211–239. https://doi.org/10.1007/978-3-319-08807-5_9

Souza, N.C.S., Silveira, J.A.G., Silva, E.N., Lima Neto, M.C., Lima, C.S., Ferreira-Silva, S.L., 2019. High CO 2 favors ionic homeostasis , photoprotection , and lower photorespiration in salt - stressed cashew plants. Acta Physiologiae Plantarum 1–14. https://doi.org/10.1007/s11738-019-2947-1

Vítolo, H.F., Souza, G.M., Silveira, J. a G., 2012. Cross-scale multivariate analysis of physiological responses to high temperature in two tropical crops with C \n 3 and C \n 4 metabolism. Environmental and Experimental Botany 80, 54–62. https://doi.org/10.1016/j.envexpbot.2012.02.002

Wang, C.-W., Wong, S.-L., Liao, T.-S., Weng, J.-H., Chen, M.-N., Huang, M.-Y., Chen, C.-I., 2022. Photosynthesis in response to salinity and submergence in two Rhizophoraceae mangroves adapted to different tidal elevations. Tree Physiology 42, 1016–1028. https://doi.org/10.1093/treephys/tpab167

Wang, W., Yan, Z., You, S., Zhang, Y., Chen, L., Lin, G., 2011. Mangroves: Obligate or facultative halophytes? A review. Trees - Structure and Function 25, 953–963. https://doi.org/10.1007/s00468-011-0570-x

Werner, A., Stelzer, R., 1990. Physiological responses of the mangrove Rhizophora mangle grown in the absence and presence of NaCl. Plant, Cell and Environment 13, 243–255. https://doi.org/10.1111/j.1365-3040.1990.tb01309.x

Yan, Z., Wang, W., Tang, D., 2007. Effect of different time of salt stress on growth and some physiological processes of Avicennia marina seedlings. Mar Biol 152, 581–587. https://doi.org/10.1007/s00227-007-0710-4

Zhou, M., Diwu, Z., Panchuk-Voloshina, N., Haugland, R.P., 1997. A Stable Nonfluorescent Derivative of Resorufin for the Fluorometric Determination of Trace Hydrogen Peroxide: Applications in Detecting the Activity of Phagocyte NADPH Oxidase and Other Oxidases. Analytical Biochemistry 253, 162–168. https://doi.org/10.1006/abio.1997.2391

Ziotti, A.B.S., Silva, B.P., Sershen, Lima Neto, M.C., 2019. Photorespiration is crucial for salinity acclimation in castor bean. Environmental and Experimental Botany 167, 103845. https://doi.org/10.1016/j.envexpbot.2019.103845

587

588